Title
Visualization of transcriptional dynamics in the early Drosophila embryo

Author
Esposito, Emilia Esposito

Publication Date
2016

Peer reviewed|Thesis/dissertation

Visualization of transcriptional dynamics in the early *Drosophila* embryo

by

Emilia Esposito

A dissertation submitted in partial satisfaction of the

Requirements for the degree of

Doctor of Philosophy

in

Molecular and Cell Biology

In the

Graduate Division

Of the

University of California, Berkeley

Committee in charge:

Professor Michael Levine, Chair

Professor Nipam Patel

Professor Donald Rio

Professor Lewis Feldman

Spring 2016

Visualization of Transcription Dynamics in the early *Drosophila* Embryo

Abstract

Visualization of transcriptional dynamics in the early *Drosophila* embryo

by

Emilia Esposito

Doctor of Philosophy

in

Molecular and Cell Biology

Professor Michael Levine, Chair

Living organisms come with building instructions, but we still do not understand them.

To the observer it is immediately visible that an elephant and an ant are very different animals. However, when observed at a molecular level, we realize that they share a comparable basic machinery of development. This concept is essentially true for all the animals, either vertebrates or invertebrates.
Over the years, different biologists tried to explain how phenotypic diversity is created, to conclude that living beings are made of similar genetic material. However, the instructions that drive their development may vary considerably.
To make a simple comparison, we can combine the same ingredients to form multiple types of food. For example, we can mix flour, salt, water and a bit of yeast to make pizza dough. The same ingredients can be used to make bread or savory cookies. The final products depend on the quantity ratio among these ingredients, the preparation, cooking strategy and the time we allow for each of these products to develop consistency and flavor.
Similarly, the same genes may lead to the formation of various cell fates just because they are expressed (or not) at different levels or different time in that specific cell. But what does regulate when, where and how much a particular gene is expressed? In other words, where can we find the manual that instructs on how organism form and develop?
When in the sixties, Jacob and Monod described that in bacteria the Lac operon transcription is controlled by non-coding elements positioned right upstream the gene (Jacob & Monod 1961), no one would imagine that a similar process would regulate gene expression in eukaryotic cells. It took about two extra decades to discover that also in eukaryotes some non-coding DNA elements were able to enhance the activity of a gene (for a complete review on enhancer discovery, see

Schaffner 2015). Contrarily to bacteria, these elements, called enhancers, were functioning in any orientation and also on a distance. At the same time, it was discovered that enhancers contain binding sites for activator and repressor proteins (Lewis 1978). Thus, a gene could be either active or inactive depending on whether activators (or repressors) were bound to its enhancer. When all the genes of a multicellular organism are expressed at the right place, time and in the right quantity, development proceeds normally.

Regulation of gene expression is far from a static process; on the contrary it is characterized by a series of dynamic events. The amount of regulatory proteins changes constantly among cells and even within the same cell. To complicate things further, enhancers can be found everywhere in the genome, often, far away from the gene they regulate. More over, DNA is a very mobile molecule and acquires multiple conformations that potentially could prevent, or favor, protein accessibility to regulatory domains and interaction between enhancers and genes.

Until recently, most of the information about gene expression derived from experimental analysis in fixed biological samples, using for example *in situ* hybridization assays that allow detection of nuclear and cytoplasmic mRNA. This technique has been useful to understand the spatial information of gene expression. Yet, in fixed samples it is very challenging to deduce the dynamic changes that occur in a developing embryo.

The continuous advancement in the molecular biology field, improvements on the visualization and computational techniques, allow now seeing and analyzing biological processes occurring in real time at increasingly higher resolution. This, together with collaborations among people with different expertise, represents a multi-disciplinary task force to understand the rules that govern gene regulation and, to a large extent, how multicellular organisms are produced.

In this thesis I intend to discuss how newly developed imaging techniques allow to push our knowledge forward about gene regulation dynamics. I will present three instances in which we reveal subtle mechanisms that fine tune mRNA production in *Drosophila melanogaster* embryos. Gene regulation is a pervasive feature that underlies the formation of all living beings and I believe that by being able to observe and analyze how biological processes occur in real-time *in vivo* we will, to some extent, be able to comprehend how life is generated.

This thesis consists of four chapters. In the first introductory chapter I present the background on gene regulation and imaging techniques. In particular I focus on the bacteriophage MCP-MS2 system since this has been my elective way to visualize transcription. In the following chapters I discuss my work done in collaboration with several bright people to visualize transcriptional dynamics

during the hours that precede gastrulation in the *Drosophila* embryo. I present how transcription occurs in burst of expression in a pair-rule gene (chapter 2), describe the existence of post-mitotic transcriptional memory (chapter 3) and, in the forth chapter, I report the analysis done to understand how transcriptional repression regulates gene activity during the formation of the mesoderm-ectoderm boundary. In this work we provide evidence that mitotic silencing facilitates repression and we suggest a model whereby repressor exploit pauses in transcriptional activity to ensure rapid gene inactivation.

List of Content

List of Figures

To Ekin, the perfect partner for my many adventures.

And to my greatest fan club:
my parents Antonio and Isabella and my sister Laura.

Chapter 1

Introduction

1.1 Overview

The decision of how and when a cell acquires a specific identity begins with the choice of turning on or off specific genes. Ultimately, the differential expression of proteins and RNAs defines what will be the final cell-type, the fate, of a developing cell. In this context, regulation of transcription plays a pivotal role in orchestrating the development of multicellular organisms. In response to some signal (internal or external), transcription factors need to access regulatory elements dispersed in a highly compact genome and activate (or repress) transcription at that locus. Contextually RNA Polymerase II (Pol II) is recruited to the promoter and released on the gene body to produce RNA. At any time, these processes are highly regulated. For example, the process of initiation, whereby Pol II is recruited to the promoter, was thought to be the most regulated step in transcription. Transcription cannot happen if the Pol II is not engaged at the gene promoter. However, genome wide assays have shown that the downstream step of transcription elongation is also highly regulated (Muse et al. 2007; Gilmourt & Lis 2009; Kwak & Lis 2013). While elongating, Pol II encounters numerous obstacles such as nucleosomes or bound proteins that might stall Pol II by impeding its movement. Despite many transcription factors that facilitate Pol II passage along the gene in its chromatin environment have been described, it is still unclear how those factors regulate transcription elongation in the context of development. Also, we now know that for some genes transcription is not continuous but cycles between period of activity (burst) and inactivity (Singh et al. 2010; Suter et al. 2011; Dar et al. 2012). Whether transcriptional bursts are functional for the developmental program of a cell is still unknown. Lastly, cell fate decision usually depends on the regulated activation and repression of multiple genes (Levine & Davidson 2005).

I am interested in understanding how those fundamental properties of transcription control development in a multicellular organism. In the specific, I want to be able to understand the dynamic processes that take place to regulate gene expression.

1.2 Experimental system: *Drosophila* embryo, an ideal model organism to study transcription regulation.

Drosophila is easy to breed, highly prolific, tolerant to diverse environmental fluctuation and has a short generation time, making it an ideal model organism for genetic studies. However, it is the *Drosophila* early embryo, prior to gastrulation, that provides a powerful model for investigating the regulatory mechanisms of cell fate specification during development. Most of the developmental programming is known. The gene regulatory network controlling the system is well mapped (Levine & Davidson 2005). We know who the critical genes are, when and in which order they interact with each other. Two morphogens gradients, control the dorso-ventral (DV) and anterior-posterior (AP) patterning (Fig. 1.1 A-B). In the ventral region, high levels of the protein Dorsal activate genes that will form the mesoderm. Progressively lower concentrations of Dorsal induce the activation of neurogenic ectodermal genes, which limit the expression to the dorsal ectodermal genes (Fig.1.2). Similarly, a broad gradient of the protein Bicoid induces the expression of several genes along the anterior-posterior axis. (For brief reviews of the DV system Hong, D. A. Hendrix, et al. 2008 and AP system Lipshitz 2009)

Extensive whole genome studies have identified transcription factors binding sequences and where Pol II binds in the genome (Markstein et al. 2002; Stathopoulos et al. 2002; Muse et al. 2007; Zeitlinger et al. 2007) In this way, and via genetic manipulations, most of the regulatory regions that control gene expression in the embryo have been characterized (Stanojević et al. 1989; Jiang et al. 1991; Ip et al. 1992; Ochoa-Espinosa et al. 2005; Zinzen & Papatsenko 2007; Kvon 2015). More over, many genetic engineering techniques permit to selectively perturb gene dosage by adding or removing genes, we can create synthetic constructs and stably integrate them into the *Drosophila* genome and test their expression profile. In addition, the first 3 hours of embryogenesis are perfectly suitable to study transcription because development is fast, synchronous and the superficial localization of the nuclei makes the embryo easily accessible to the observer via light microscopy (Coppey et al. 2007; Coppey et al. 2008). Not only, the small size of the embryos allows high-throughput experiments. We can for example label a gene in hundreds of embryos and image all of them at the same time. Being able to observe numerous samples with the same experimental condition provide good statistics and quantification of the population variability and not just of the single organism. And finally, many imaging techniques are available to precisely visualize and quantify gene expression. We can for example visualize single molecule mRNA per nucleus or following transcription in vivo via the MS2-MCP system in many nuclei simultaneously (Garcia et al. 2013; Lucas et al. 2013).

1.3 Seeing is believing. The progress of visualization techniques. "Once upon a time…Life" was a French-Japanese-Swiss-Italian animated TV series produced in the nineties with the educational purpose of showing how the human body works and what are its components. The show was imaginary set inside the human body and the spectator could see how cells and molecules interacted within each other. The biological world was animated to make it visible so that an amateur could understand it.

In a somewhat similar way, a scientist tries to obtain data that allow visualizing, at least in an abstract way, a connection, a causative link, a mechanism, that may be beneficial to describe and understand what happens in the real world. To do so, scientists need to develop and use the appropriate technology. Hypothetically, one day we will be able to devise a small camera that travels in any cell of a living organism and show in real time what is happening in any single part of the body. Let us imagine this camera going into a human body. We are composed of about 50 trillion cells. With the exception of the germline, each cell contains 23 pairs of chromosomes that are structures of highly packaged DNA and proteins. If we consider that the human haploid genome contains about 3 billions of base pairs of DNA, and that each base pair is about 0.34 nanometer long, one human contains 100 trillion meters of DNA. In comparison, the earth circumference is only about 40000 kilometers. Now imaging to see, as it happens, this massive machine of DNA moves inside all these cells, is replicated, transcribed into RNA and produce the molecules that safeguard its self-sustenance and help the cell to grow. If such a devise existed, we would take part to the cellular concert of highly coordinated events that creates life. Indeed, the limit of our understanding is closely related to the limit of the experimental techniques available.

Currently it is not possible to simultaneously visualize all the events occurring in all the cells of an organism in real-time. However, the continuous advancement of technologies yielded to new tools that permit direct visualization of gene expression in living cells. Until recently, gene regulation was studied mainly fixed samples. Techniques such as RT-PCR, chromatin immunoprecipitation, transcriptomics and mRNA *in situ* hybridization provide useful information about protein and DNA interactions, how much, where and when mRNA is produced; yet they represent mere snapshots of what is happening in the cell at the time of fixation. In some cases, it is possible to reconstruct the temporal and spatial progression of an event by examining multiple samples and identifying the precise developmental stages (Lagha et al. 2013). However, here transcriptional dynamics would be the result of a cell population average and our analysis might be lacking of transitory events. Gene expression is not a static process; rather it is dynamic and can rapidly change in response to various stimuli and regulatory events (Phair & Misteli 2001; Misteli 2008).

To overcome these limitations, a substantial advancement came from the combination of fluorescent proteins and the protein-nucleic acid interaction system of bacteria and bacteriophage. For example, to visualize DNA in living cells, we can insert the bacterial Lac operator sequence (LacO) in any genomic location of our preference using genetic engineering (Rafalska-Metcalf et al. 2010; Rafalska-Metcalf & Janicki 2013). Following, the co-expression of the Lac repressor (LacI) fused to a fluorescent protein binds to its operator and permit real-time visualization. A similar result can be obtained by using the parABS system (Saad et al. 2014). These techniques have been very useful to learn the binding kinetic of transcription factors to DNA and to study how DNA varies its topological conformation over time (Bertrand et al. 1998; Chubb et al. 2006; Darzacq et al. 2009; Hocine et al. 2013; Park et al. 2010; Eliscovich et al. 2013; Buxbaum et al. 2014).

A new method, adapted the bacteriophage unique RNA hairpin sequence MS2 and the MS2 coat protein (MCP) to enable time-lapse imaging of mRNA dynamics and localization in living cells. Here, multiple MS2 repeats are cloned into the mRNA of our choice. Upon transcription, the RNA sequences of MS2 form a series of stem and loop repeats that are recognized by the MCP fused to a fluorescent protein (Fig.1.3). Homologous systems using cognate hairpin–coat proteins are now available, such as the phage PP7-PCP, the λ-phage N-protein–boxB system as well as the U1A mRNA labeling system; although the latter cannot be used in mammalian cells (Fig.1.4). For a complete review see (Weil et al. 2010). The presence of so many variants allows to simultaneously imaging multiple mRNA and to integrate information at a more complex level.
To add value to the newly developed labeling systems, light-microscopy techniques are constantly trying to improve the physical limits of resolution and sensitivity. In addition, computational methods became very useful to extract meaningful quantitative information about mRNA (or protein) production, kinetics and movements inside a cell. Altogether, improvements in the genetic engineering methods, in conjunction with computational and imaging technological progresses are challenging the classical knowledge of gene expression and lead the way to the discovery of novel regulatory mechanisms.

1.4 The MS2-MCP system: benefits and limitations

The bacteriophage MS2-MCP system revolutionized the way we observe transcription. By fluorescently tagging the RNA as it is formed during transcription, we finally can observe all the dynamic processes that we had previously inferred from multiple fixed samples. The system is quite versatile. We can combine multiples hairpin loops and a variety of fluorophores to detect different parts of the same mRNA or multiple transcripts in the nucleus. We can use the fact that the MS2 interacts with the MCP to tether the mRNA of our interest to any specific protein. For example, we can fuse the MCP to a protein

present in a specific cellular compartment and in this way tether the mRNA to that compartment. Similarly we can use the MCP-MS2 system to affinity purify a transcript (Buxbaum et al. 2014). See figure 1.5 for a list of the novel uses of the MS2-like systems.

Although this approach provides unprecedented insights into the dynamics of gene expression, there are few limitations. To detect transcription, the MS2 hairpins are artificially introduced into reporter gene or in specific genomic loci. Usually, fluorescent signal is detected only when multimerized copies of the stem and loop are used (generally from 6 to 24). This allows the signal to accumulate above the background level, represented by the unbound MCPs fused to a fluorescent protein. The presence of unbound MCP constitutes a problem since it creates an inherent fluorescence background. To fine-tune the signal to noise ratio, it is therefore critical to find the right balance between MCP concentration and number of the MS2 binding sites. Expressing too little MCP is deleterious because the lack of sufficient coat protein may cause that some hairpins will not be bound. Vice versa, too much MCP will increase the inherent background. In both these condition we may underestimate transcription (Buxbaum et al. 2014; Ferraro et al. 2016).

Another limitation is represented by the artificial introduction of so many stem and loop. Large exogenous sequences might affect the transcriptional behavior of the transgene. It could for instance change the chromatic state of the locus or affect the mRNA processing and lifetime. It is not known for example whether Pol II transcriptional rate is influenced by the stem and loops. Another thing to consider when using this system is the location of insertion of the stem and loops. In fig. 1.6 is reported the fluorescence outcome of three transgenes in which the MS2 cassette was inserted in the 5' UTR, 3'UTR or intronic region. The insertion in the 5'UTR produces the strongest signal. Here fluorescence is detected as soon as transcription begins and accumulates along the whole transcription unit. The main problem related to this location is that the fluorescent signal persists upon termination, until all the mRNA is on the gene body. Also the 5' region corresponds to the ribosomal entry; thus the MS2 in this location may affect translation. In the 3'UTR the fluorescent intensity signal is low. More over, we will detect a delay between the onset of transcription and signal detection when the MS2 is in this location. The delay is proportional to the gene length and Pol II elongation rate (Ferraro et al. 2016). By placing the MS2 in the intron we will also detect a delay. In this case, the delay depends on where the intron is located in respect to the transcription start site. In this location, persistence of the signal depends upon the splicing process. Since splicing can be either co-transcriptional or occur after transcription, the MS2 in the intron may not accurately reflect transcription.

A

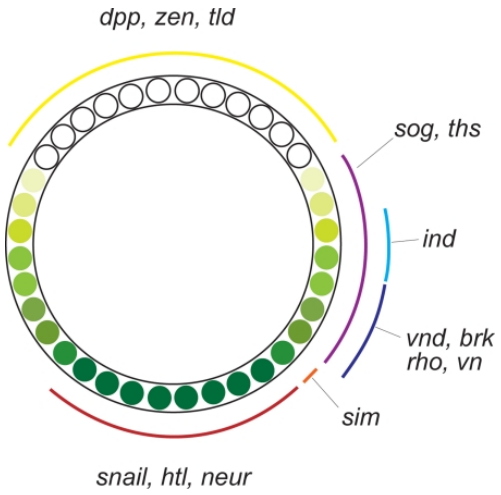

B

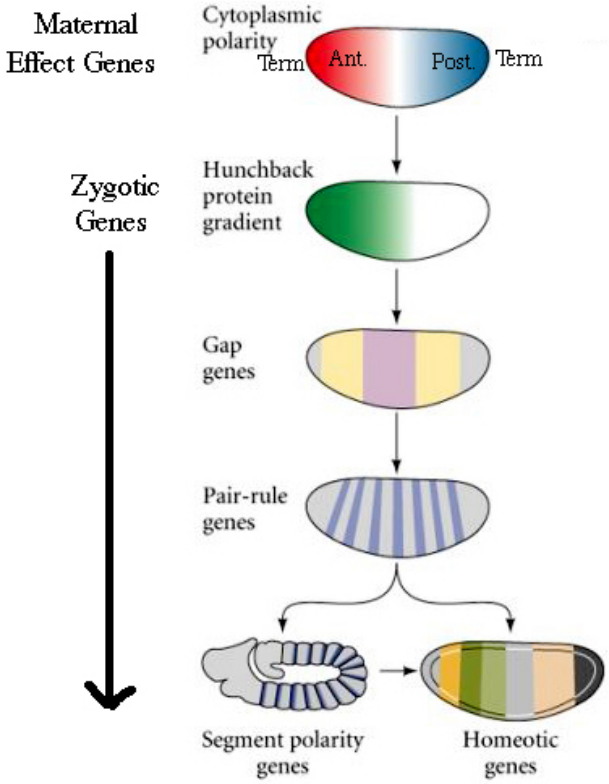

Figure 1.1: *Drosophila* patterning systems (A) Schematic cross-section of an embryo showing the Dorso-Ventral patterning regulators (reproduced from Hong, D. A. Hendrix, et al. 2008) (B) Formation of the anterior-posterior axis (reproduced from the biology course at Utah university)

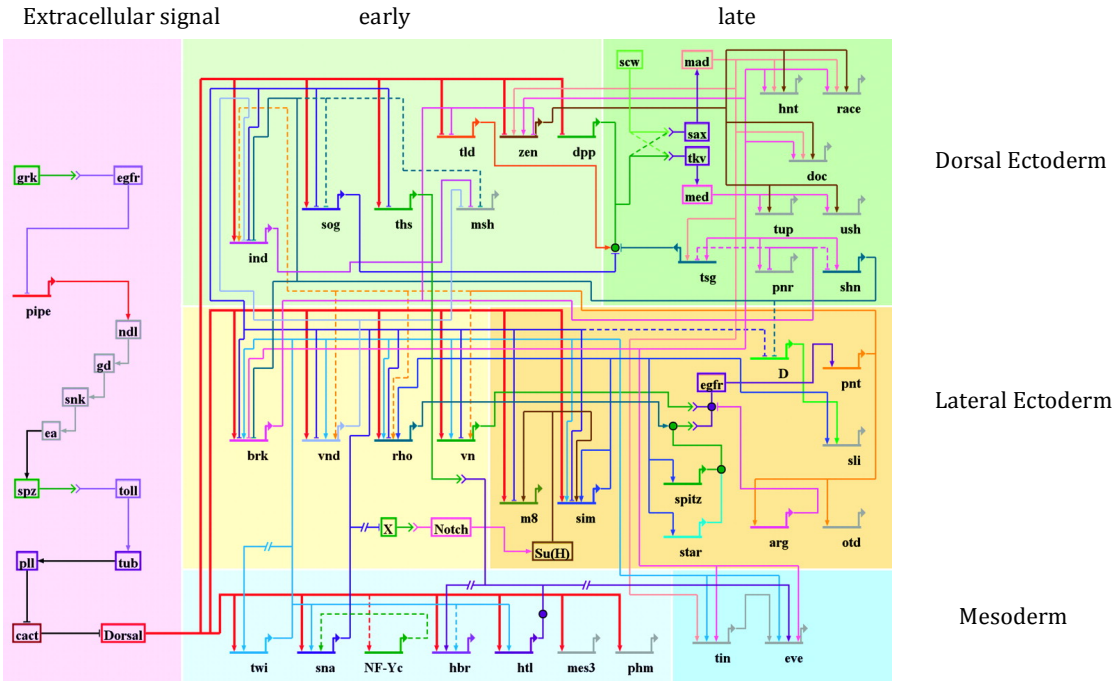

Figure 1.2: The Dorso-Ventral patterning Gene regulatory network (reproduced from Levine & Davidson 2005)

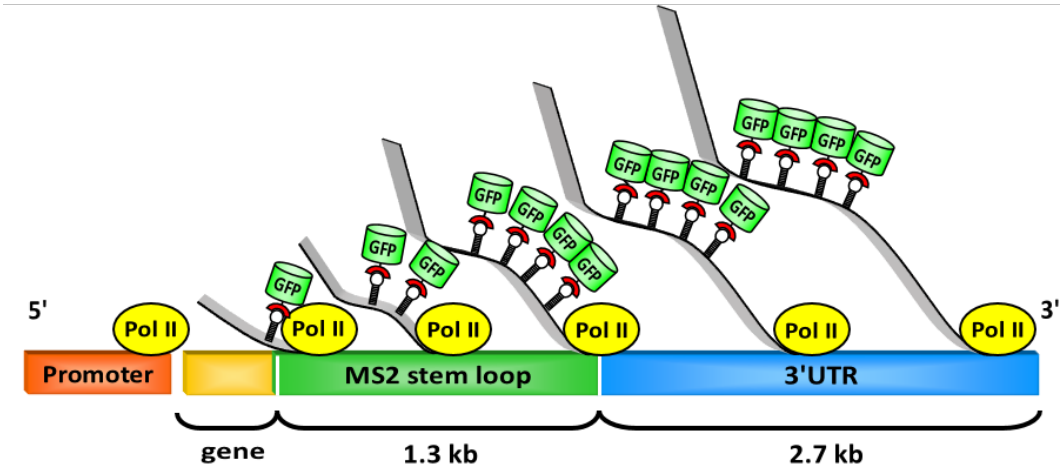

Figure 1.3: Schematic representation of the MS2-MCP system. The MS2 stem and loop is added to a gene of interest. Upon transcription the MS2 hairpin form and can be recognized bt the MS2 Coat protein fused to a fluorophore (in the picture GFP). (reproduced from Yuval Garini laboratory)

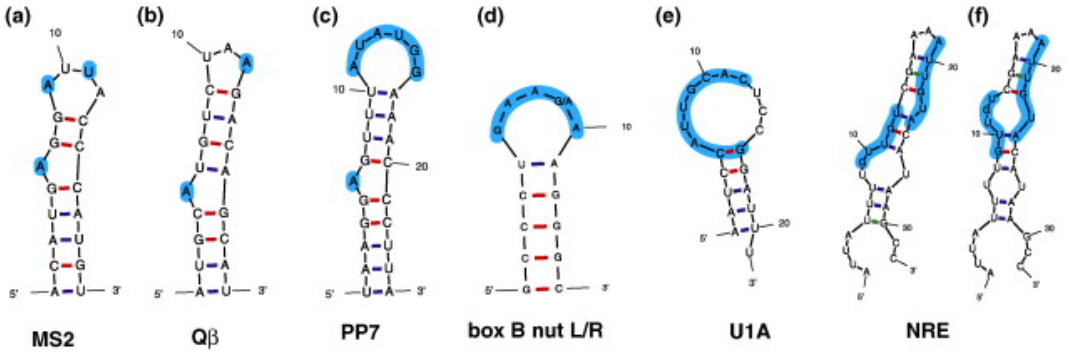

Figure 1.4: Schematic representation of the various RNA hairpins adapted to visualize transcription. (Reproduced from Weil et al. 2010)

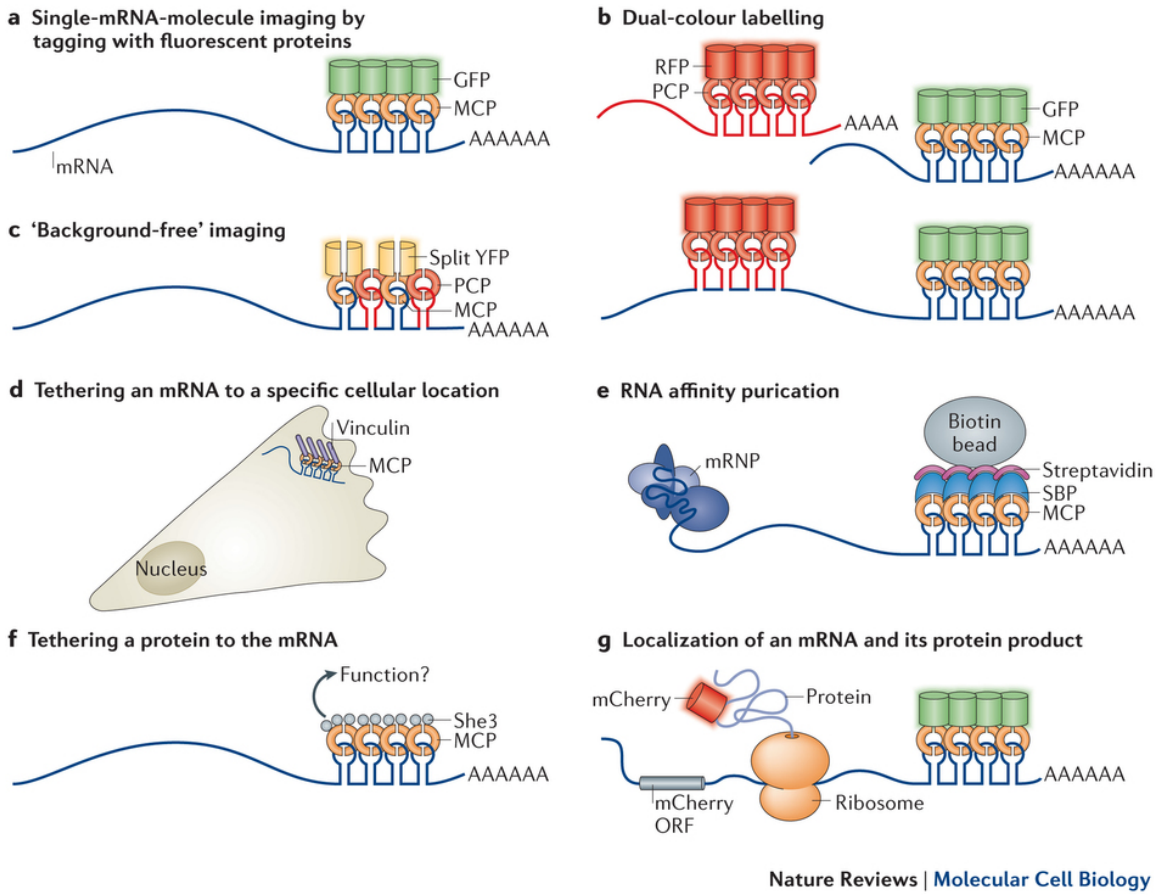

Figure 1.5: Multiple uses of the MS2-like systems (Reproduced from Buxbaum et al. 2014) (A) Classical use of the MS2 to visualize mRNA formation (B) two different stem and loops are used to visualized different mRNA simultaneously (C) split GFP is used to reduced the MCP inherent background. In this system MS2 and PP7 hairpins are alternate to each other. Their respective coat proteins (MCP and PCP) are fused to different halves of a split fluorescent protein. Upon transcription, the MCP and PCP bind to adjacent locus and the fluorescent protein become functional. (D-E-F) MCP can be fused to protein to perform several functions. In D, MCP is fused to a specific cellular compartment. This allows MS2 to re localize. In E the MCP-streptavidin complex can be affinity purified using biotynilated beads and in F we can tether a protein to the mRNA to observe its function. (G) Simultaneous localization of mRNA and the protein. The protein can be visualized by fusing the gene to a fluorescent protein or via novel tagging system (Halo-tag, snap-tag)

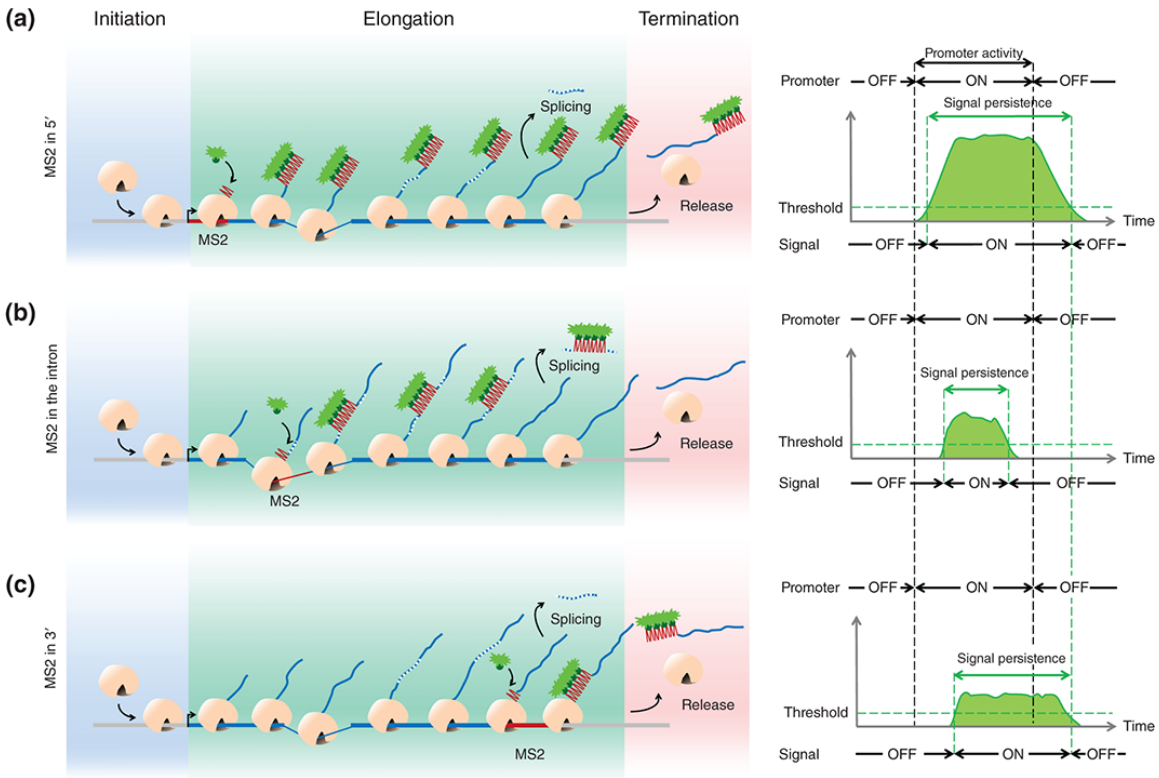

Figure 1.6: The location of the MS2 stem and loops within the transcription unit influences the signal intensity and its persistence. (Reproduced from Ferraro et al., 2016)

Chapter 2

Transcription can be discontinuous

2.1 Overview

Cell fate specification and survival depend on the correct expression of many genes. Transcription of a DNA sequence into an mRNA product is the first step that regulates when and where a gene becomes active and how much of it is produced. Any mistake at this step might potentially lead to cellular phenotypes due to over- or down- producing a specific factor. In order to understand how transcription is regulated, scientists face the challenge of finding accurate measurement of transcriptional activity. Gene expression in single cells is highly variable and sporadic. For example, studies in Drosophila and mammalian cell lines revealed the existence of two kinetics of gene activation (Boettiger & Levine 2009; Lagha et al. 2013). Some genes are activated with a similar kinetic in all the nuclei where the enhancer is active, leading to a synchronous pattern of activation. On the contrary, another class of genes is characterized by a less coordinated activation producing a more "salt-and-pepper" pattern. It is still unclear what are the mechanisms that control the temporal dynamics of gene expression and how transcriptional heterogeneity arises. Many studies suggested that stochastic gene expression can be generated when transcription fluctuates between ON and OFF states (Rajala et al. 2010; Suter et al. 2011; Larkin et al. 2013; Wang et al. 2012). Thus, discontinuous transcription might explain why in a region where the enhancer is active, some nuclei show transcription while others do not.

In growing organisms, these measurements become increasingly more difficult given the mutable nature of genes in responding to multiple stimuli that cause expression to change over time. Recent improvements in imaging and computational method have permitted to visualize and quantify transcription in real-time in living embryos (Garcia et al. 2013; Lucas et al. 2013).

Here I described the work I did in collaboration with Gavin Schlissel, a graduate student during his rotation period in the Levine lab, Jacques Bothma, during his postdoctoral studies in the Levine lab, and Hernan Garcia, during his postdoctoral studies in Thomas Gregor lab at Princeton University. The analysis of the expression pattern of *eve* revealed that transcriptional burst influences the stripe formation. Our work was published in the journal PNAS in 2014 (Bothma et al. 2014)

2.2 Material and Methods

2.2.1 Fly Genetics

Female virgins maternally expressing MCP-GFP and Histone-RFP from (Garcia et al. 2013) were crossed with transgenic males containing the eve>MS2-yellow

construct. Collected embryos were imaged using either of two-photon or confocal microscopy.

2.2.2 Cloning and Transgenesis

Plasmid construct was built using the pbPHi backbone vector containing *yellow* reporter gene (Venken & Bellen 2007; Perry et al. 2011) The eve region containing eve enhancer and promoter region (-1.7 kb,+50bp) was amplified from genomic DNA using the following primers:
atttgcggccgcCAAGAAGGCTTGCATGTGGG
cgggatccAACGAAGGCAGTTAGTTGTTGACTG.
24 repeats of the MS2 stem loops were extracted from plasmid pCR4-24XMS2SL-stable (Addgene 31865) by digesting with BamHI and BglII. This fragment was ligated into the *eve-yellow* pbPHI vector linearized with BamHI. The MS2 tag was inserted immediately upstream of the yellow reporter gene coding sequence (the ATG of the yellow ORF is mutated to avoid translation of this late gene at early embryonic stages). This strategy permits an enhancement of the signal since MS2mRNA (and therefore GFP binding) will be present as soon as Pol II reaches this sequence and will be maintained until Pol II reaches the polyA sequence, 6kb downstream of the MS2 first loop. Eve>MS2-*yellow* plasmid was integrated on chromosome 3 (Vk33).

2.2.3 Fluorescent *In Situ* Hybridization and microscopy

2-4 hr *yellow;white* (*yw*) embryos were fixed as described by Kosman et al. (2004) Bothma et al. (2011) Hapten-tagged RNA probes were used for hybridization. Embryos were imaged on a Zeiss 700 laser scanning microscope in z-stacks through the nuclear layer at 0.5µm intervals using a Plan-Apochromat 20x/0.8. Confocal images were captured at 2048x2048 pixel resolution and at 8 bit color depth.

2.2.4 Confocal time-lapse microscopy

Embryos were collected 2-3 hours post fertilization and mounted for imaging as described in Garcia et al. 2013. Embryos were imaged on a Zeiss 780 confocal microscope using a Plan-Apochromat 40x/1.4NA. Fifteen z-stacks were captured spanning the nuclear layer spaced 0.7µm, and images were captured at 512x512 or at 1024x1024 pixel resolution. For wide-field microscopy, the pixel size was X (1024x1024) or Y (512x512). For high-magnification microscopy, the pixel size was Z (512x512).

2.2.5 Image processing and analysis

All image analysis was performed on the max-projection of z-stacks. Nuclei were identified in each frame as described in Bothma et al. 2011. Nuclei were false-colored if they contain at least one focus of transcription. All image analysis was performed in Matlab.

2.2.6 Live imaging sample preparation and data acquisition

Female virgins maternally expressing MCP-GFP and Histone-RFP from (Garcia et al. 2013) were crossed with transgenic males containing the eve>MS2-yellow construct. The embryos were dechorinated with bleach and mounted between a semipermeable membrane (Biofolie, In Vitro Systems & Services) and a coverslip and embedded in Halocarbon 27 oil (Sigma).

2.2.7 Data analysis and mathematical model

Analysis was performed as described in (Garcia et al. 2013). A detailed description of the mathematical model can be found in Bothma et al. 2014.

2.3 Results and Discussion

The fate map of the adult fly is specified by several hundred patterning genes that are regulated by about a thousand enhancers during a one-hour interval of embryogenesis, between 2 and 3 hours after fertilization (Alberts et al. 2002).
We now understand that the spatial constrain that regulate patterning are controlled by the regulatory protein that bind to enhancers. However, the information concerning the temporal dynamic is still lacking.

2.3.1 Construction of eve>MS2 transgenic fly.

We decided to visualize the pattern formation of the *even-skipped* (*eve*) gene driven by the stripe-2 enhancer. *eve* encodes a homeodomain transcriptional repressor (Macdonald et al. 1986; Frasch & Levine 1987) which has a primary role during segmentation, when the embryo became subdivided into repetitive regions – or segments – distinct by a specific cell fate. *In situ* hybridization data have shown that, prior to cellularization, in nc 14, *eve* expression pattern consist of 7 stripes that partition the blastoderm (Frasch & Levine 1987). This pattern corresponds exactly to the odd segments of the embryo and mutations that affect *eve* expression cause, in fact, the loss of alternating segment boundaries (Nüsslein-Volhard et al. 1985). The 7 stripes are regulated independently by a series of separate enhancers (Goto et al. 1989; Harding et al. 1989; Small et al. 1992). This modularity is achieved thanks to the action of short-range repressors that efficiently inhibit expression in a particular stripe, but do not interfere with the others.
We chose to study eve stripe-2 enhancer since it is one of the best-characterized elements during animal development (Levine 2010). *eve* stripe-2 contains 12 binding sites for regulatory protein: 6 for the activators Bicoid (Bcd) and hunchback (hb) and 6 for the repressors Giant (Gt) and Krupper (Kr), (Fig. 2.1 A) (Small et al. 1991; Stanojevic et al. 1991; Arnosti et al. 1996). The maternal protein Bicoid is distributed in a broad gradient with peak levels in the anterior and low expression at the posterior region of the embryo. In the anterior most region of the embryo, high levels of Bcd activate the gene hunchback (*hb*). Upon activation, Hb and Bcd bind synergistically the *eve*-stripe 2 enhancer and activate its expression in a broad region in the anterior half of the embryo. Subsequently,

the repressors, Giant in the anterior and Kruppel in the posterior, refine the expression domain of *eve* to establish the final border of the stripe 2 (Surkova et al. 2008).

We were curious to study the temporal dynamics of *eve* stripe-2 refinement and wondered whether we could obtain insight in its regulation by live imaging analysis.
For this reason we created a transgenic reporter-gene containing 24 repeats of the MS2 stem and loop and a yellow reporter gene driven by a 1.7 kb long DNA sequence located upstream the *eve* endogenous promoter (Fig. 2.1 B). This region contains eve promoter region as well as the entire 720 base pairs (bp) of *eve* stripe-2 enhancer. It also presents some weak regulatory elements that control expression of stripe 7.
This transgene was stably integrated into the Chromosome 3 of a *Drosophila* strain and transcription was visualized in real-time via confocal or two-photon microscopy (see material and methods).
To investigate whether our *eve*>MS2 transgenic embryos recapitulate the spatial limit of *eve* stripe 2 in the endogenous locus, we stained a transgenic embryo using probes against *eve* endogenous mRNA and a full-length probe against the yellow reporter gene by conventional fluorescence in situ. In fig. 2.1C it is possible to observe that the staining pattern of our reporter gene and *eve* endogenous stripe 2 overlap, indicating that the presence of the MS2 cassette is not an issue for the transcriptional regulation of *eve*.
We then crossed *eve*>MS2 male transgenic flies to flies loaded with a maternal protein driving the expression of the MS2 coat protein (MCP) fused to GFP (MCP::GFP), to visualize the fluorescence signal in real-time movies. These flies also contain histones tagged with RFP on Chromosome 2 that allow nuclei detection (Garcia et al. 2013) .Movies of living Drosophila syncytial embryos were taken over the course of 3 hours, from nc 11 to gastrulation at the end of nc 14.
Still-shots from one of the movies are shown in figure 2.1 D. Broad expression is detected in the anterior half of the embryo during early nuclear cycle up to nc 13. In nc 14, the stripe gradually refines and ultimately disappear prior to gastrulation (Fig. 2.1 D panel f). The dynamic of the stripe-2 pattern, namely broad activation followed by localized repression in the anterior and posterior region of the embryo is consistent with previous studies of fixed embryos.

2.3.2 what new insight can we obtain by the analysis of living embryos?

The first striking observation is that the stripe formation is way more dynamic than expected from fixed studies. The mature stripe pattern is very transient and last about only 15 minutes of the ~90 minutes that eve>MS2 is active. Interestingly, we also noticed a marked refinement of the pattern following the nc13/nc14 mitosis (Fig. 2.2). During nc13, *eve* is transcribed in a broad pattern, throughout most of the length of the embryo. We calculate that at this time *eve* is expression covers 10% to 70% egg length (Fig. 2.2A, D). However, at the onset

of nc 14, *eve* expression domain is significantly restricted in the posterior region, where the repressor Kruppel is expressed. At reactivation, *eve* is transcribed between the 20% and 40% egg length (Fig. 2.2 B-D). This domain is significantly broader than the final limits of the stripe-2 pattern, but considerably more restricted than the pattern observed at preceding stages. We hypothesize that Kruppel repressor somehow has the ability to exploit the general loss of transcription that occurs during mitosis. Further evidence of a link between mitosis and patterning will be discussed in chapter 4.

Once the restricted domain of reporter gene expression is established following nc 13/nc 14 mitosis, a gradual refinement of the stripe 2 continues, indicating that Gt and Kr repression continues during interphase to establish the final limits of the stripe. By the midpoint of nc 14, a definitive stripe 2 pattern is observed, but it rapidly disappear within 15 minutes after formation. The analysis of fixed preparation suggested a more stable stripe, but the analysis in vivo reveals that the pattern is instead highly dynamic and it is continuously changing and refining.

2.3.3 Analysis of the data reveal transcriptional burst.

One of the biggest advantages of using live fluorescence data is that we can extract the fluorescence intensity signal of transcribing loci and employ computational analysis to monitor and calculate the amount of mRNA molecule produced per nucleus over time. The amount of fluorescence signal is proportional to the amount of Pol II transcribing the gene and hence it offers the possibility to have instantaneous measurement of gene activity (Garcia et al. 2013).

To understand when the mature stripe forms, we false colored the active nuclei according to the fluorescent intensity signal detected over the course of nc 14. At the beginning of nc 14 nuclei express variable levels of the transgene (Fig. 2.3 D-E). Only towards the end of the nuclear cycle, when the stripe refines, the mature stripe of steady state become apparent (Fig. 2.3 F). When we plotted the fluorescence intensity traces obtained for single nuclei over the course of nc 14 we realized that transcription was highly discontinuous, in other words it fluctuated between periods of high activity and periods of low or no activity (Fig. 2.4). Discontinuity of transcription reveals the existence of transcriptional bursting, whereby periods of gene activity (bursts) alternate with periods of inactivity. Transcriptional bursts have been reported in other systems subject to live-image analysis, including bacteria, yeast, Dictyostelium and cultured mammalian cells (For review see Lionnet & Singer 2012). There are evidences that some genes exhibit a continuous transcription profile in which transcription possesses the same kinetic over time. For example, two independent laboratories (Gregor Lab at Princeton University in the USA and Dostatni Lab at the Marie Curie Institute in France) showed that from nc 11 to the first 20 minutes of nc 14, hb>MS2 transgenes display a stable and continuous expression in the anterior 40% of the embryo, and during this time there is a only a little dynamic

change, mostly at the boundary (Garcia et al. 2013; Lucas et al. 2013). Maybe, sustained transcription of Hunchback transgene correlates with its stable pattern of expression; on the other side, transcriptional bursting allows for the constant changes in the *eve* pattern.

Living imaging offers the opportunity to predict the amount of mRNA produced over time for each nucleus and thus model the behavior of transcriptional activity. Because of changes in the fluorescence intensity are proportional to the amount of Pol II on the gene body, we can extrapolate the rate of Pol II loading at the promoter. For example, from the moment transcription starts we will detect an increment of fluorescence that scales linearly with the amount of Pol II present on the gene. If Pol II is loaded at a constant rate, when the first Pol II reaches the end of the gene the fluorescence intensity will be at a steady equilibrium because new Pol II will be loaded onto the gene. This equilibrium results in a stable intensity that will change once the gene is switched off. At this time the amount of Pol II falling off the gene are greater than Pol II on the gene and thus we will detect a diminishment of the fluorescence signal (Fig.2.5 A-B). Using a mathematical model, we detected that mRNA production cycles between periods of activity ranging from 4 to 10 minutes. This result suggests that between 20 and 100 molecules of mRNA are produced per transcriptional per burst, suggesting that bursts may be associated with the highly dynamic pattern observed. Our prediction is comparable to the amount of mRNA obtained and burst durations observed in other systems (Lionnet & Singer 2012). Interestingly, our observation indicates that Pol II loading changes over time from a minimum of 4 Pol II per minutes to 14. This result suggest that bursting is not a passage between an ON and OFF state at a constant rate, but it favors a multi state model in which many variables influence the kinetic of mRNA production. For a detailed description of multistate model see Jenkins et al. 2013)

2.3.4 Conclusions

Our analysis indicated that the classical stripe pattern is transient, highlighting the importance of additional enhancers in the *eve* regulatory region for maintaining the stripe during gastrulation and germ band extension (Harding et al. 1989; Goto et al. 1989). The Kruppel repressor is more efficient than Giant in the formation of the stripe borders. There are numerous possible explanations for these differential rates of repression. First, mitosis might assist transcriptional repression. There is very little reactivation of the eve>MS2 transgene after the onset of nc4 where there are high levels of Kruppel repressor. During mitosis, the transcription machinery and most of the transcription factor are released from the chromatin. Perhaps mitotic silencing offers an opportunity for Kruppel to bind and maintain the gene in an inactive state. Repression following mitosis may be more efficient for Kruppel than Giant because in the anterior region high levels of activator could effectively compete with the repressor for binding after mitosis. This is not the case for the posterior region where Bcd and Hb levels are limiting.

In a second model, Kruppel may remain associated with its target sites on condensed mitotic chromosomes, similar to the persistence of a pioneer factor during mitosis (for review see Zaret & Carroll 2011). If so, Kruppel could prevent the activators Bcd and Hb from productively binding to the enhancer at the onset of nc14. Alternatively, it is possible that transcriptional bursting facilitates the regulation of *eve* stripe 2. Perhaps repressors are more effective during the off phases of *eve* bursts. *Vice versa*, enhancers mediating constant pattern of transcription, such as the Hb proximal enhancer, may be more refractory to repression as compared with those producing bursts. Future experiments may help to test this hypothesis by examining the vast spectrum of enhancers and their transcriptional dynamics.

In the next chapters I examined how mitosis impacts transcription. I will first describe the existence of transcriptional memory and in the last chapter I will discuss the link between mitosis and Snail repression during the neurogenic ectoderm pattern formation.

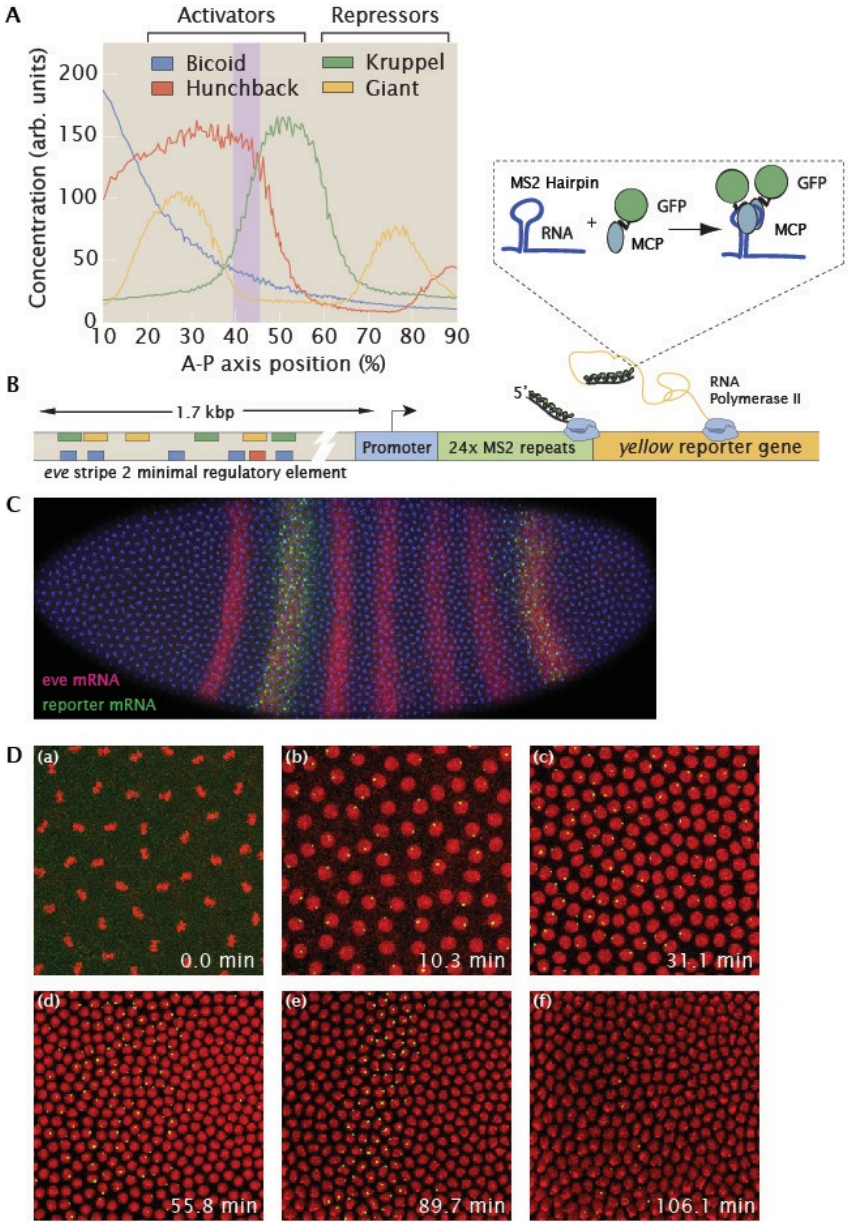

Figure 2.1: Expression pattern of the *eve* stripe 2 transgene.

(A) Schematic representation of the regulation of *eve* stripe-2 enhancer. (B) Schematic representation of the eve>MS2 plasmid. The binding domains for the regulatory protein in A are shown in the same color. (C) Fluorescent in situ hybridization staining of a Drosophila embryo in nc 14 showing eve endogenous gene (magenta) and eve-stripe 2 transgene (green). Nuclei are stained with DAPI (blue). (D) snapshots of movies taken at the confocal microscope show the refinement of the *eve* transgene over time.

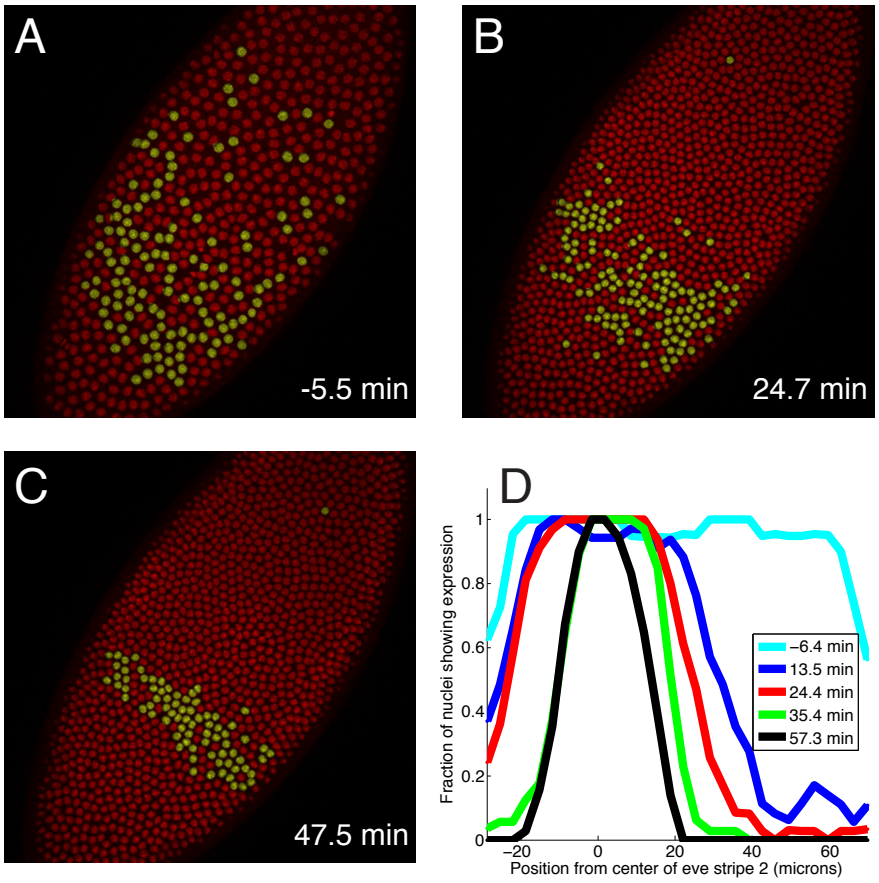

Figure 2.2: refinement of the *eve* pattern after mitosis
(A-C) Projected confocal stacks of a live embryo expressing eve>MS2 at different time points. Nuclei are false colored in red (His-RFP, transge is not expressed) and yellow (transgene is active). (A) *eve* expression pattern in nc13. (B-C) Expression pattern at two time points in nc14. It is evident that eve pattern refines between the two nuclear cycles. (D) Analysis of the fraction of active nuclei in relationship to the center of the stripe. Negative values indicate time before nc13/nc14 metaphase, positive values correspond to time after mitosis. In nc 13 eve expression pattern is very broad (light blue line), upon mitosis we calculated a drastic refinement in the posterior region (dark blue line)

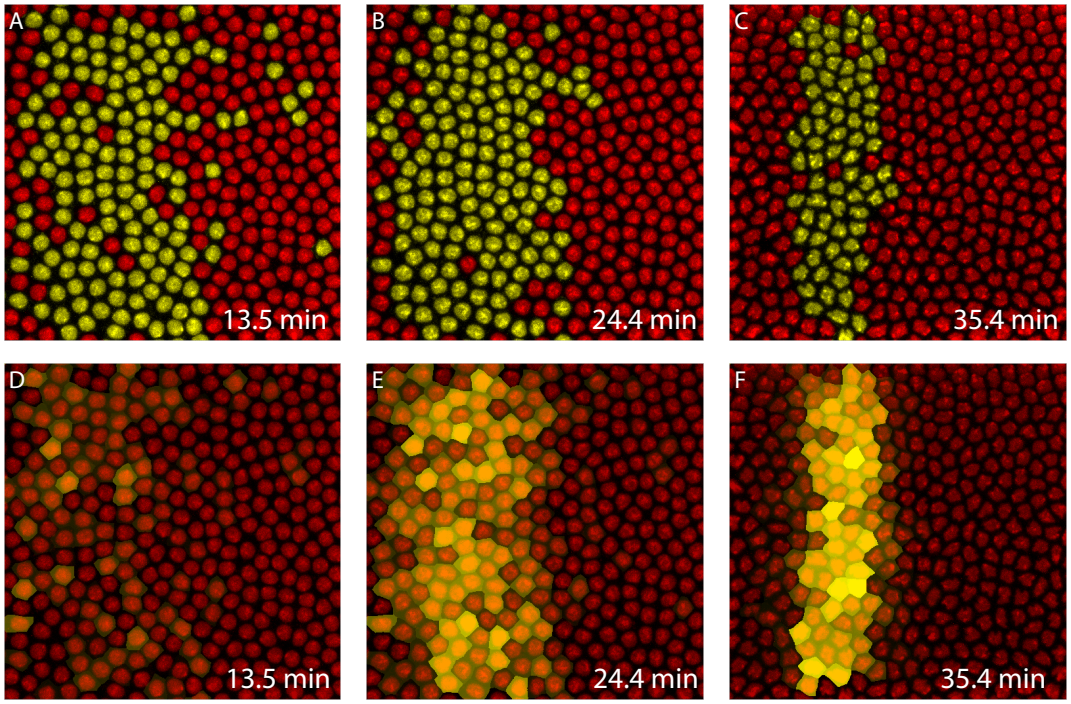

Figure 2.3: *eve* pattern is highly variable in nc 14.
(A-C) snapshots of movies taken at the confocal microscope show the refinement of the *eve* transgene over time in nc 14. Active nuclei are false colored in yellow. (D-F) The images in panel A-C are false colored in shades of yellow by integrating the total fluorescent signal as function of time. Stronger yellow color indicates higher fluorescent intensity signal. This signal is proportional to the amount of mRNA produced in each nucleus. Eve expression increases during nc 14, but nuclei are characterized by a great variability in their expression levels. Towards the end of nc 14, *eve* stripe refines and present the same limits as the stripe observed with conventional *in situ*. The mature stripe is characterized by higher transcriptional output than the border regions.

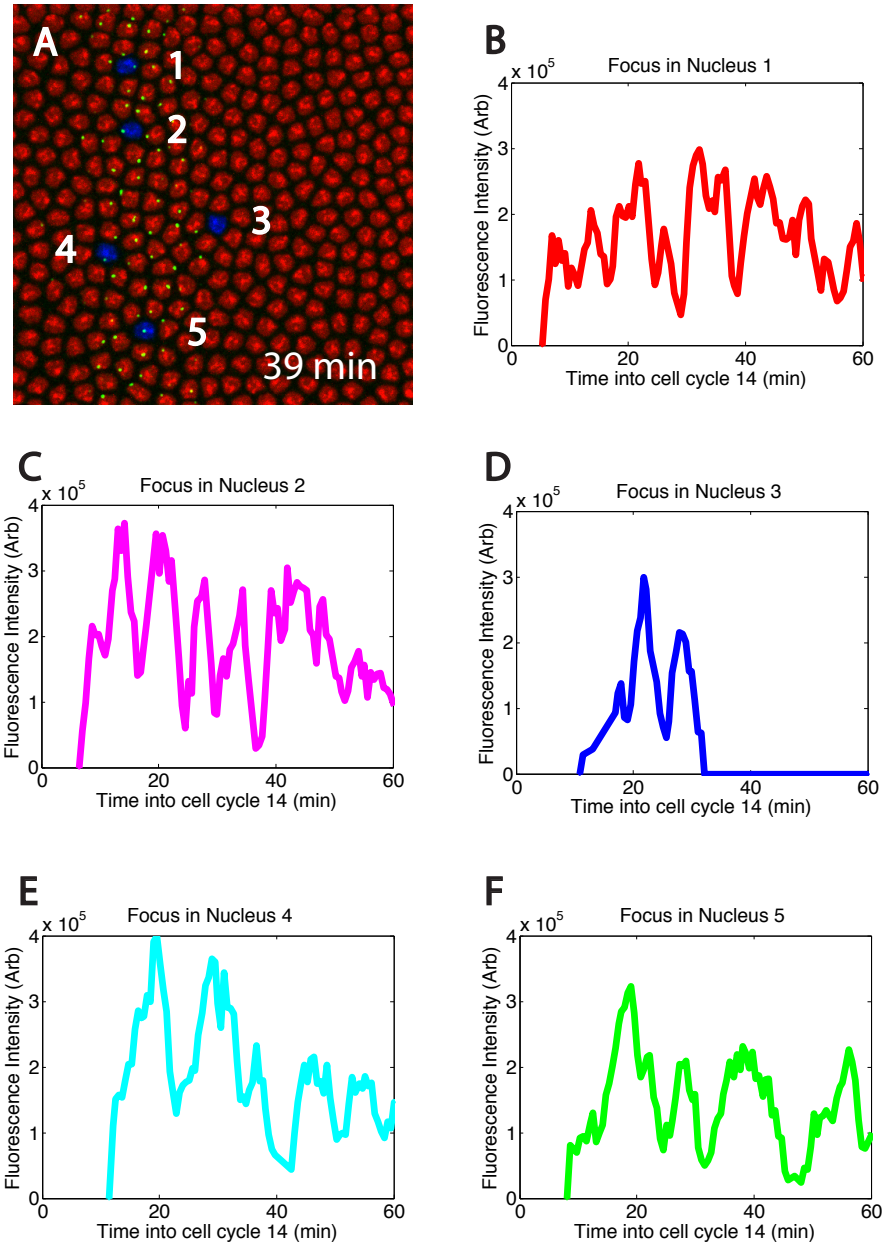

Figure 2.4: single fluorescent Intensity traces indicate the existence of transcriptional bursts.
(A) Projected confocal stack of a live embryo in nc14 showing the mature *eve* stripe 2. In blue are false colored the nuclei whose single traces are analyzed in panel B-F. (B-F) Fluorescent Intensity profile of multiple nuclei located in different region of *eve* pattern. Single traces indicate that transcription is not continuous, and reveal the presence of transcriptional bursts.

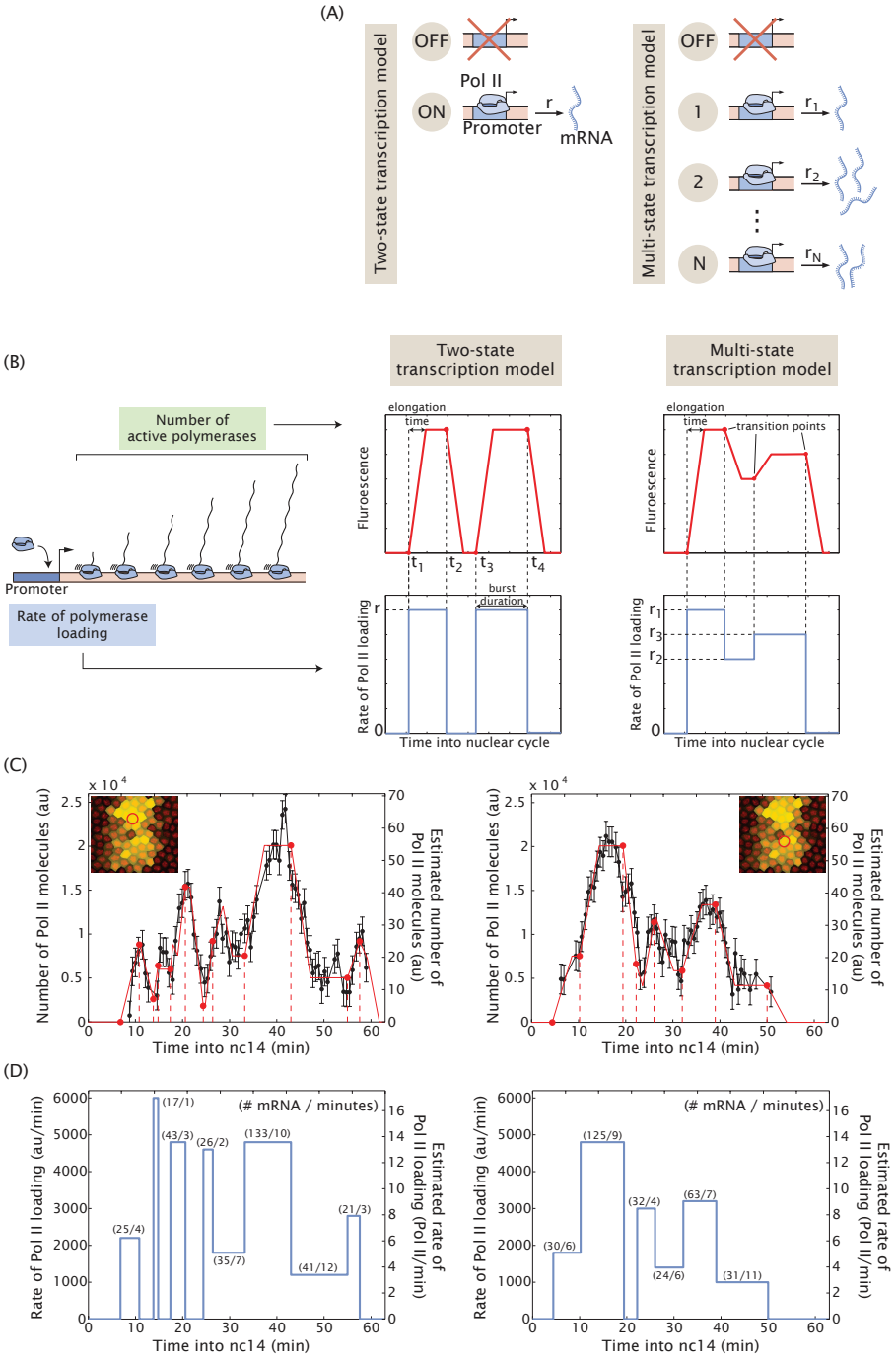

Figure 2.5: Transcriptional bursting activity of eve stripe 2
(A-B) Description of the two state transcription model and the multi-state transcription model. In the first model, transcription fluctuates between an ON and an OFF state, where by the promoter is active or silent. Transcription factors can regulate how frequently these two states switch or the rate of transcriptional initiation. In a multistate model, the promoter is characterized by different initiation rates between pulses. For example Pol II loading may vary every time the promoter is active. (C) Fluorescence intensity trace of a single nucleus within *eve* stripe. Two nuclei are displayed. (D) Manual fit of the fluorescence traces in C display an estimation of the rate of Pol II loading over time.

Chapter 3

Transcriptional memory in the Drosophila embryo.

3.1 Introduction

If you are curious to know who your ancestors are, you will probably start with what you know about yourself and your history. You will probably build your family tree, using your parents, grand parents and immediate family members. For most of the people it will be easy to build a family tree because they will have record or direct experience of who these people are. But what do we do when we do not know anything about ourselves? We may search for someone who has a memory or a story of our family; we will try to find any details related to our family that will help fill the gaps. Sometimes, a research using our last-name might help to go back in time of many generations and trace our history. A last-name is an addendum to the name, which carries additional meaning. Already during the Roman Empire, a name was given to identify people belonging to the same family. For example, by simply using my last-name "Esposito" I can trace my genealogical tree to around 1600 A.D. in an orphanage "Ospizio degli esposti" of Naples, Italy. Etymologically, Esposito derives from the word "Exposed". Tradition hands down that the children were given the last name Esposito because they were "exposed" to the public for adoption.
In our modern era, sequencing DNA is also an opportunity; and we can search for our ancestors by looking at similarity with our DNA genome.

But how does a cell know what it derived from? How does it know what it has to be? How do cells preserve expression pattern across cell-lineage and, more generally, development?
It was shown that in bacteria and yeast, certain proteins remain in the cytoplasm of the daughter cells and in this way perpetuate the genetic program active in the mother cell to its descendants (Ptashne 2008). In lambda bacteria, the lysogenic pathway involves transmission in the cytoplasm of a protein that by binding to its DNA sequence perpetuates its synthesis in the progeny. In other words, they act as a memory determinant, somewhat similarly to a last-name. In female mammals, X-inactivation represents another example of memory. Here one of the two X-chromosomes is randomly inactivated (Lyon 1961; Ptashne 2008). The identity of the inactive chromosome is transmitted to the progeny by an unknown mechanism via cell division. Again in mammals, but also in invertebrates, several studies revealed that some factors, for instance proteins belonging to the Polycomb and Thritorax complex, modify chromatin to maintain the active or inactive transcriptional status inheritable through cell division (Francis & Kingston 2001; Sadasivam & Huang 2016). Transcriptional memory could be important for the rapid re-activation of the cell transcriptional program. Indeed, live-imaging analysis in the unicellular eukaryote Dyctostelium, have shown that genes are

activated faster when they were active already in the previous cell cycle (Muramoto et al. 2010; Zhao et al. 2011).

The cell fate of Drosophila is specified very early during embryogenesis. In the first hours after fertilization maternal cues activate a series of zygotic genes essential for defining the body patterning of the future fly. Rapid and synchronous mitosis produce an embryo of around 6000 nuclei in which patterning genes need be precisely express to avoid developmental defects. How does the embryo achieve such precision? Redundant genetic network, redundant enhancers and/or redundant genes confer robustness to genetic and environmental perturbation or stressful condition (Perry et al. 2010; Perry et al. 2011), the presence of paused polymerase promote a synchronous transcriptional activation within cells (Boettiger & Levine 2009; Lagha et al. 2013). These are just few mechanisms that have been shown to 'fine-tune' the spatial and temporal control of gene expression and foster developmental precision. Transcriptional memory might definitely be another mechanism that contributes to the accurate cell fate specification.

3.2 Background

During the first years of my graduate studies, I worked extensively with a postdoctoral student Mounia Lagha and a graduate student Jacques Bothma to study the dynamics of patter formation of the gene *snail (sna)*. We focused on *snail* because it encodes for a transcription factor that is essential for epithelial-mesenchyme transitions (EMT) in most of all animal systems (Wang et al. 2013) and in Drosophila Snail protein is a key element to ensure proper gastrulation (Hemavathy et al. 2004). Snail expression is highly regulated. The endogenous *snail* locus exhibits activation during nuclear cleavage cycle 10, shortly after the migration of zygotic nuclei to the cortex of the egg, ~75-90 min following fertilization. At each of the ensuing 4 mitotic divisions, snail transcription is silenced and reactivated during successive interphases. After the 13th nuclear division *snail* transcription is maintained for the entire 1-hour interval of nc 14, which culminates in the invagination of the mesoderm at the onset of gastrulation. During nc14, *snail* transcription is very synchronous, whereby most of the nuclei are activated around the same time (Boettiger & Levine 2009; Lagha et al. 2013). A previous work indicated that *snail* contains a redundant, shadow, enhancer that helps buffering environmental and genetic stressful condition (Perry et al. 2010). Mounia, Jacques and myself revealed that Pol II pausing affects the temporal kinetics of *snail* pattern (Lagha et al., 2013). Thus, the replacement of the *snail* promoter with the promoter of a non-paused caused stochastic activation of *snail* expression and resulted in an increased variability of mesoderm invagination. The temporal dynamics of *snail* was inferred using multiple images of fixed preparation of Drosophila embryos covering nc 13 and nc 14, therefore we could not test whether transcription kinetics was remembered throughout mitosis.

What happen when the normal mechanisms of regulatory robustness and precision are disrupted? To address this question we created a minimal, defective *snail* distal enhancer and employed the MCP-MS2 system to visualize its expression in living embryos. Here I discuss the methods we used and the results of our research published in the journal Current Biology in 2016 (Ferraro et al., 2016). Our work indicates the presence of transcriptional memory in the early *Drosophila* embryo. Myself, Laure Mancini and Mounia Lagha designed the experiment and imaged the embryos. The computational analysis was performed by Teresa Ferraro, a postdoctoral student in biophysics at the Curie Institute, France.

3.3 Material and Methods

3.3.1 Fly Genetics

Virgin females expressing maternal MCP-GFP and Histone-RFP were crossed to homozygous transgenic MS2 males as described in Garcia et al. 2013. The resulting embryos are heterozygous for the MS2 transgene. To obtain homozygous MS2 transgenic embryos, homozygous MS2 males were crossed with MCP/MS2 virgin females. Both the MS2 transgene and MCP::GFP transgene are integrated on chromosome 3 (VK33 *Drosophila* strain).

3.3.2 Live imaging

Embryos were dechorionated with a tape and mounted between a hydrophobic membrane and a coverslip as described in Lucas et al. 2013. Time-lapse images were taken using an LSM780 Zeiss confocal microscope with the settings described in Bothma et al. 2014. The GFP and RFP proteins were excited using a 488nm and a 561nm laser respectively. All the acquisition are taken in a central ventral region of the embryo, zoomed at 2.1.

3.3.3 Cloning and Transgenesis

A pbPHI-MS2 vector was obtained as described in Bothma et al. 2014. All transgenic flies were obtained by injection into VK33 lines in the Levine lab.
snail enhancer: a 500bp fragment from the distal snail shadow enhancer and minimal promoter sequences (100-150 bp) from the *sna, sog, ilp4, scp2, wntD* and *brk* genes were amplified using the following primers:

snaE-Fwd: 5'-CCTTGGTCCTACCTTCG- 3'
snaE-rev: 5'-CCAAAGGCAACGCCGATTTCC- 3'.
Scp2Pr-Fwd: 5'-ACTGCGATAAGATAAAGC- 3'
Scp2Pr-Rev: 5'-TTTCTGATTAAATTTTGGTAC- 3'
ilp4Pr-Fwd: 5'-AATACGTGAAGTCAAAAAGTCAATAG- 3'
ilp4Pr-Rev : 5'-TGGCAAACCGATCGCTGGGCATGC- 3'
brkPr-Fwd : 5'-AGGCGAGGCAGTCTAGAACG- 3'

brkPr-Rev: 5'-TCATAACTCGCGTTTGCGATC- 3'
wntDPr-Fwd: 5'5CTGGCTTGGGATTTGCAGG-3'
wntDPr-Rev: 5'-TATATTGTTGTTATGGTGCTATC- 3'
sogPr-Fwd: 5'-GCCGTTGCATGTTGCCG- 3'
sogPr-Rev: 5'-GATCGTATCGTATCGTA- 3'
snaPr-Fwd: 5'-GACAGCGGCGTCGGCAG- 3'
snaPr-Rev: 5'-TGGTTGCGTTCTCAACG- 3'

CAGE data was used to determinate the TSS (Hoskins et al. 2011). When the annotated TSS differed from that obtained by CAGE, 5'-Race on 2-4h embryonic extracts was conducted (for e.g. *ilp4* promoter).

3.3.4 Fluorescent *in situ* hybridization

Fluorescent in situ hybridization was performed as described in Lagha et al. 2013. A dixogygenin-MS2 probe was obtained by in vitro transcription from a bluescript plasmid containing the 24-MS2 sequences, isolated with BamH1/BglII enzymes from the original Addgene MS2 plasmid (# 31865).

3.3.5 Image processing and analysis

Image processing of the MS2-MCP- GFP signal was performed as in Lucas et al., 2013.

3.3.6 Manual analysis of homozygous movies:

Nuclei of embryos homozygous for snaE>snaPr-MS2 transgene were manually tracked (three movies). We focus on the active mother nuclei at nc13 with two clear dots, and tracked the lineage of these nuclei over mitosis. We then examine the descendants of these homozygous active mothers at 5min into nc14 and 10min into nc14 and count the various combinations, symmetric (2,2) and (1,1) or asymmetric (1,0); (2,0) and (2,1).

3.3.7 Segmentation and Tracking of the MS2-MCP- GFP spots.

Spot localization and segmentation is performed on the maximal projection of the z-stacks for each time frame. After noise filtering, spots are localized by setting a threshold on the fluorescence level at 1.5 fold of the average background level. The spots are then tracked across time frames. For extended procedure see Ferraro et al., 2016.

3.3.8 Average Activity. The transcriptional activity is measured as the sum of the fluorescence intensities in each connected pixel forming a spot at a given time. The average activity corresponds to the temporal average of the activity starting two minutes after the initiation time. This data produces an estimation of the regime transcription rate of a spot.

3.3.9 Integral Activity. It is an estimate of the total mRNA produced by a given spot during the entire time ON. It is calculated by summing the activities across all the time frames and it is linearly related to the total amount of mRNA produced by a given spot.

3.3.10 Random model.
A mathematical model was computed to calculate the temporal behavior of active nuclei coming from active mothers in the absence of memory bias. For the mathematical formula see Ferraro et al., 2016.

3.4 Results and discussion

3.4.1 Construction of a stochastically expressed plasmid to study memory

To study whether transcriptional memory existed in the early Drosophila embryo, we created a minimal, defective *snail* enhancer and employed the MCP-MS2 system to visualize its expression in living embryos. We decided to perturb the *snail* distal enhancer since its regulation was well known to create an enhancer that mediates slow and sporadic activation of MS2 reporter genes in living embryos.

The precellular embryo is ideally suited for such studies since it is naturally synchronized; all of the nuclei are at the same stage of the cell cycle. Moreover, each embryo contains hundreds of nuclei, thereby providing statistical power even when small numbers of embryos are analyzed. Imaging and computational analysis of the stochastic activation profiles seen for the sensitized *snail* transgene led us to the observation of transcriptional memory. That is, transcription of the transgene in one cell cycle predisposes for the rapid re-activation in the next cell cycle following general silencing during mitosis. This memory is normally obscured by the transcriptional robustness seen for the endogenous *snail* locus.

The full-length shadow enhancer is about 1.5 Kb long and contains a core region of multiple binding sites for the activators Dorsal and Twist encompassing a region of 500 bp. It also contains binding sites for the protein Zelda and an extra twist-binding domain (Fig. 3.1 A). The protein Zelda is implicated in timing the maternal-to-zygotic transition and many studies suggest that its binding correlates with the timing of activation (ten Bosch et al. 2006; Nien et al. 2011; Rushlow & Shvartsman 2012). For our analysis, we decided to use the small 500 bp core region containing the activators sites, but lacking Zelda and the extra twist (Fig.3.1 A). We reasoned that by removing the Zelda binding region, we would likely affect the timely activation of the endogenous *snail* during early stages of development. This minimal enhancer was placed immediately upstream 100 bp flanking the transcription start site of snail and 24 repeats of the MS2

stem and loop were added downstream the promoter to maximize detection of the fluorescence signal.

Fluorescence *in situ* hybridization and real time movies indicate that *sna* minimal enhancer is able to recapitulate *snail* endogenous pattern but, as predicted, is characterized by a much slower kinetic and stochastic expression (Fig. 3.2 A-D).
We do not detect transcription of the MS2 cassette before nc 13. During nc 13 the MS2 signal is detected in just few nuclei. After the mitotic silencing, transcription resumes in just a fraction of the nuclei in the mesoderm. It takes about 30-40 minutes to visualize transcription in all the nuclei of the mesoderm, while the full-length enhancer takes about 10 minutes to fill the pattern. Imaging and computational analysis allowed us to trace the lineage of nuclei in nc 13. In our analysis, transcriptional memory is defined by the higher likelihood to become active soon after mitosis in the nuclei that descended from active mothers (for a schematic representation see Fig. 3.1 B).
At reactivation in nc14 after mitosis, the first cohort of nuclei to become active derived from active mothers (memory nuclei) (fig.3.1C). These nuclei correspond to the 2% of the final pattern of expression. During the next few minutes, 27 more nuclei became active (9% of the pattern). Among these, more than a half (15/27) were descendent of active mothers (Fig. 3.1C, 3.3 A-A'). As nc 14 continues, more nuclei become active and many of them arise from mothers that did not transcribe the transgene during nc13 (non-memory nuclei). This is not a surprise considering that by the end of nc 13, only 10-20% (26/175) of the mesodermal nuclei showed *sna* expression (Fig.3.1C, 3.3). Nonetheless, statistical analyses provide clear evidence for memory (summarized in Fig. 3.3 A' – B') indicating that, in average, the daughters of memory nuclei were four times more likely to display re-activation at the onset of nc 14 compared with the daughters of non memory nuclei. To avoid bias, we modeled the probability of activation in the absence of memory, assuming a binomial sampling of a constant fraction of active nuclei in each nuclear cycle. Our analysis showed that the observed transcriptional memory was significant. In fact, the number of active nuclei coming from active mothers at the onset of nc 14 was always greater than the expected value if activation was random (Fig. 3.3 C).

3.4.2 Transcriptional memory is independent of the promoter sequence.

From the analysis on paused Pol II, we knew that the promoter architecture affects the temporal kinetics of gene expression (Lagha et al., 2013); therefore we were curious to understand whether the promoter sequences could also have a role in memory.
We repeated the experiment using a different set of promoters that contain Pol II pausing, *brinker* and *ilp4*, or that lack Pol II pausing *wntD* and *scp2*. Quantitative analysis shows that depending on the promoter we used, between 60% to 80% nuclei originated from memory nuclei in the first 5 minutes of nc 14 (Fig. 3.3 A-A'-B-B', E). The promoter sequences thus influences the efficiency of

transcriptional memory. The *snail* and *ilp4* promoters yield a higher efficiency of reactivation during the initial phases of nc14 than the *wntD* promoter (Fig. 3.3 E). However, we did not observe any significant correlation between memory and promoter elements, as the presence of TATA box, or levels of Pol II pausing does not correlate with the amount of memory nuclei produced. For instance, *scp2* (non-paused, TATA box) and *brk* (paused, no TATA box) give rise to comparable amount of memory nuclei. The basis for these differences is uncertain, but might scale with the duration of transcription during nc13.

3.4.3 What is the mechanism of transcriptional memory?

DNA sequences may remember that they were transcribed in a previous cycle thanks to some mitotic bookmarking. Transcriptional bookmarking have been previously reported through nucleosome displacement or histone modifications, to name some (Zhao et al. 2011). According to this hypothesis, after mitosis the nucleus that would have inherited the transcribed template may be more susceptible to re-activation. Another possibility considers asymmetric distribution of activators between daughter nuclei. Although the embryo is a syncytium where proteins can diffuse, small variations in their local concentration are possible. These slight changes may cause some nuclei to have higher levels of activators and produce an asymmetric activation of the MS2 transgene.

To test the latter hypothesis we analyzed the inheritance pattern of neighboring nuclei focusing our attention to the central part of the *snail* domain where activators are at peak levels. At the boundary region, limiting amount of activator may mislead our analysis because it would be easier to create asymmetry between nuclei (Fig. 3.4 A).

Our analysis shows that, in general, a memory nucleus is activated twice as faster than a neighbor nucleus coming from an inactive mother (Fig. 3.4 B). More over, we observe a delay in the activation time between sister nuclei. This delay is higher among non-memory sister nuclei (Fig. 3.4 A, C). In heterozygous embryos, the fluorescent spots of sister nuclei derive from the two different chromatids of the unique transgenic allele (Fig. 3.5 A). The delay observed could be explained by different mechanisms. Perhaps activators are asymmetrically distributed during mitosis. In the nucleus that received higher concentration, transcription would start faster than the other. Alternatively, the two chromatids are differentially transcribed and the differences in expression are inherited during mitosis. Or maybe, during mitosis only one of the two chromatids is bookmarked for faster expression (fig. 3.5 C). To further test these hypotheses, we decided to observe the activation behavior of homozygous embryos.

Contrarily to heterozygous where a nucleus can be either active or inactive, homozygous embryos offer the possibility to observe different transcriptional configurations. In homozygous embryos, upon mitosis we observe mainly two different patterns of activation. Sister nuclei either express both one allele (1,1 configuration) or, with equal frequency, one nucleus is not transcribed, while in the other both alleles are active (2,0 configuration) (Fig. 3.5 B, D). If memory was

caused by asymmetric concentration of the activator levels between sister nuclei we would expect to observe more frequently asymmetric configurations such as (2,0), (2,1) or (1,0) rather than a 50-50 ratio between (1,1) and (2,0).
The simplest explanation for these observations (in heterozygous and homozygous embryos) is that only one of the two sister chromatids of the homologue chromosome experiences transcription. After mitosis, only the daughter nucleus that inherits the transcribed sister chromatid exhibits rapid reactivation, while the daughter that inherits the non-transcribed sister chromatid exhibits the same slow and variable reactivation kinetics as the daughters of non-memory mothers (summarized in Fig. 3.5 C-D). Thus, the two patterns observed are the consequence of independent assortment of sister chromatids during mitosis.

3.4.4 Does transcriptional memory help patterning the Drosophila embryo or is it an intrinsic property of transcription?

To address this question we measured the total activity of transcription produced from nuclei derived from active and inactive mothers. We wanted to determine whether memory mothers produce daughter nuclei exhibiting more efficient Pol II elongation. If this is true, transcription might be progressive, leading to increasing efficiencies in the production of mRNAs due to prior "priming" events. Memory nuclei produce about twice the amount of mRNA produced from non-memory nuclei (Fig. 3.6 A, magenta plots). However, there is not a significant difference in the levels of transcription from memory and non-memory nuclei that are activated at early time points (Fig. 3.6 A, grey plots). Overall, memory nuclei produce higher levels of mRNA products than non-memory nuclei since they are active for longer periods during nc14 (Fig. 3.6 C). However, once activated, non-memory nuclei produce about the same levels of nascent RNA signals as memory nuclei (Fig. 3.6 A-C). Moreover, nuclei that are first activated during late phases of nc14 produce the lowest levels of nascent RNAs since there is an overall reduction in the levels of snail transcription during later stages (Fig. 3.6 C). This reduction in expression during the second phase of nc14 is also seen for BAC transgenes containing all of the regulatory DNAs controlling *snail* expression in the early embryo (Boettiger & Levine 2013). Non-memory nuclei that are activated during early stages of development produce about the same total levels of nascent RNAs as memory nuclei. We therefore conclude that memory is an inherent property of transcription; in the same way that bursting is emerging as a general feature of transcription. It does not appear that memory is important for the patterning of the Drosophila embryo since endogenous regulatory loci such as *snail* tend to be robust, and exhibit rapid and synchronous activation profiles during development. However, it seems reasonable to suggest that memory might be important for the sustained and reliable expression of constitutively active "housekeeping" genes during consecutive cell cycles.

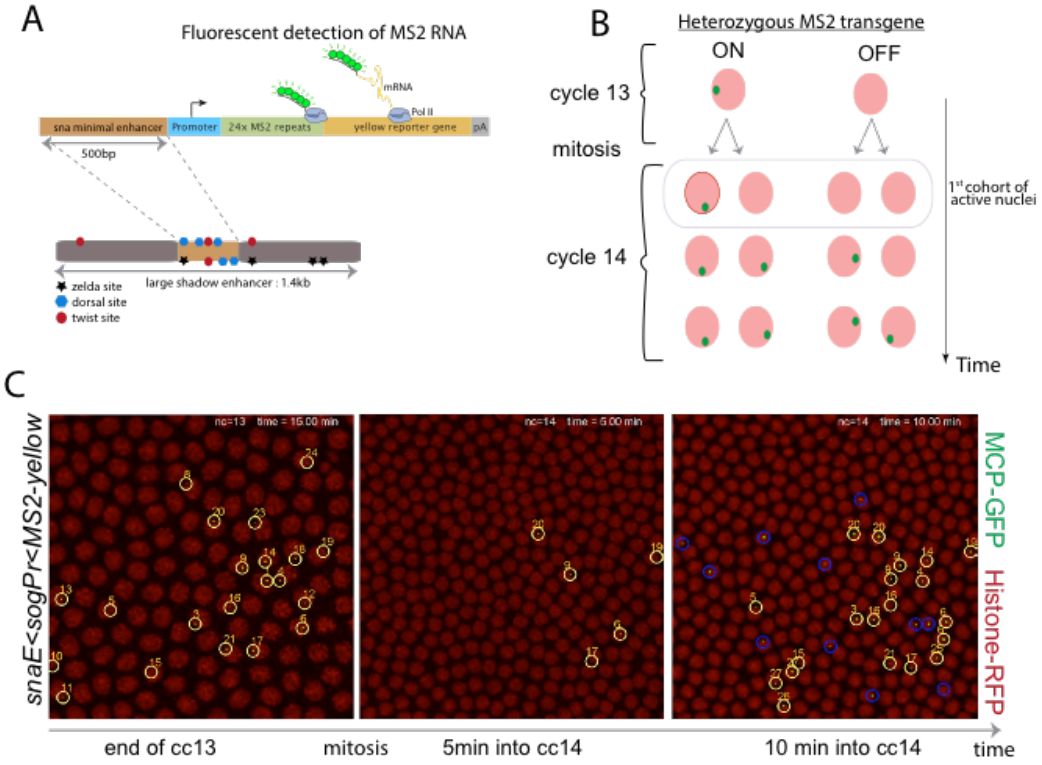

Figure 3.1: Transcriptional memory is observed in a sensitized *snail* transgene
(A-B) Schematic description of the sensitized *snail* transgene construction. (B) Cartoon indicating transcriptional memory. Daughter nuclei descending from active mother are activated faster than daughter nuclei coming from inactive mother. (C) Projected confocal images of an embryo during nc 13 and at the onset of nc 14. Active mother are circled in yellow (nc13). At reactivation in nc 14, the first nuclei becoming active descend from active mother (yellow circle). In the following 5 minutes also nuclei that derive from inactive mother start to be express (blu circle). Nuclei are in red. Transcriptional foci in green.

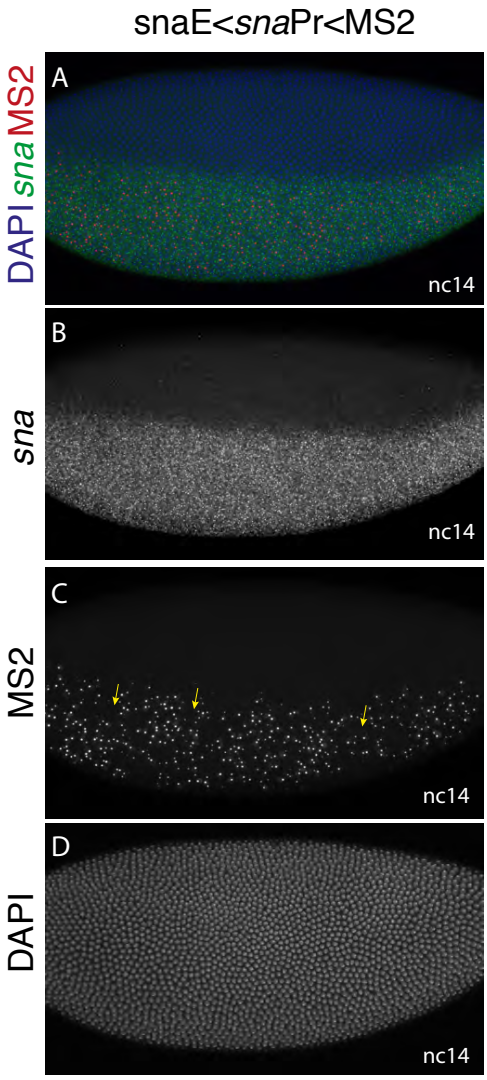

Figure 3.2: The core snail enhancer produces a stochastic pattern of expression
(A-D) Fluorescent in situ hybridization staining of a Drosophila embryo in nc 14 showing sna endogenous gene (green) and *sna* minimal Enhancer>MS2 transgene (red). Nuclei are stained with DAPI (blue). (B) endogenous snail only, (C) *sna* minimal Enhancer>MS2 transgene only and (D) DAPI channel.

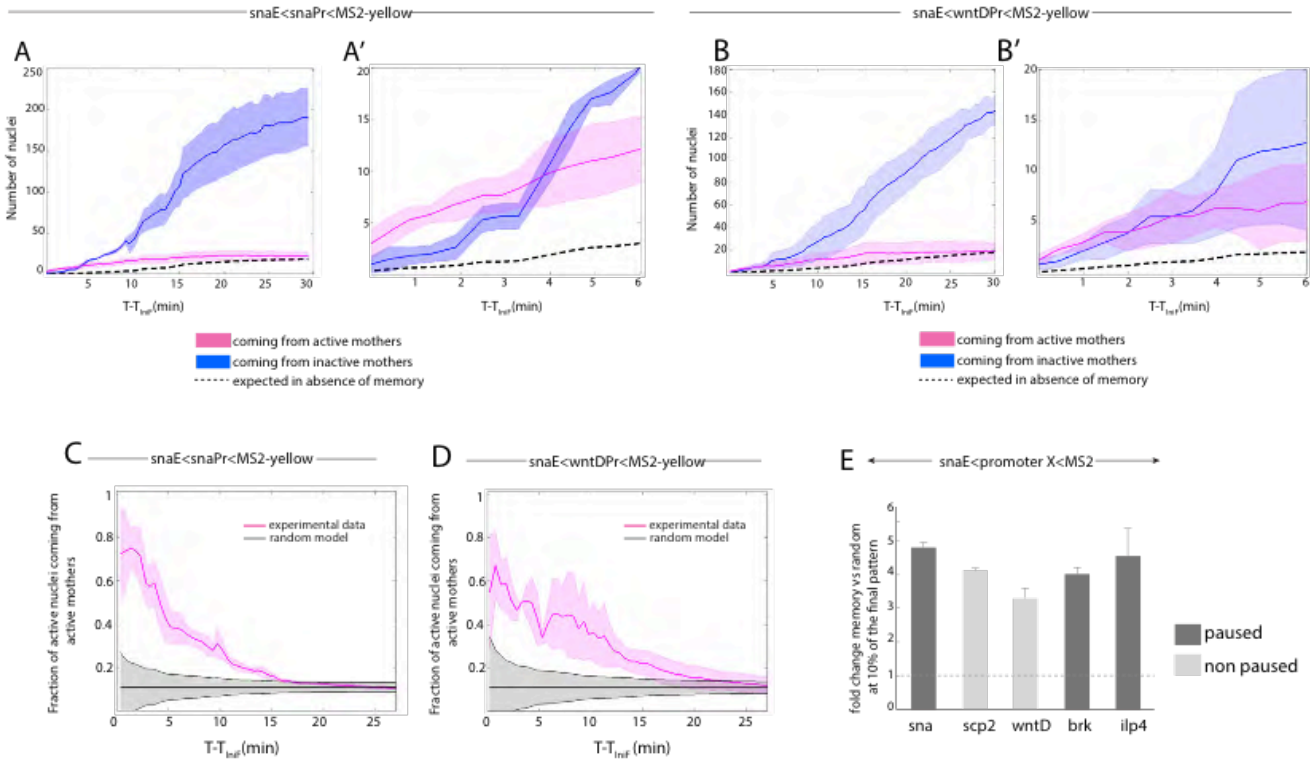

Figure 3.3: Quantitative analysis of transcriptional memory
(A-B) Activation kinetic curves (number of active nuclei over time in nc 14) calculated for memory (magenta) and non-memory nuclei (blue) of transgenic embryos expressing snaE>snaPr-MS2 (three independent movies – figures A, A') and snaE>wntDPr-MS2 MS2 (three independent movies – figures B, B'). A' and B' are zoomed in version of the first 6 minutes. Shaded area correspond to the standard deviation. (C-D) Temporal kinetic of the fraction of active nuclei coming from active mother for a paused gene (snaPr) or a non-paused gene (wntDPr) are compared to a mathematical model of random activation distribution. See Ferraro et al., 2016 for mathematical model. (E) Probability that first nuclei becoming active come from memory nuclei is calculated for 5 different transgenes (paused gene: *sna, brk, ilp4* and non-paused gene: *scp2, wntD*) dividing the observed memory nuclei by the fraction calculated with the random model. Error bars correspond to the standard error.

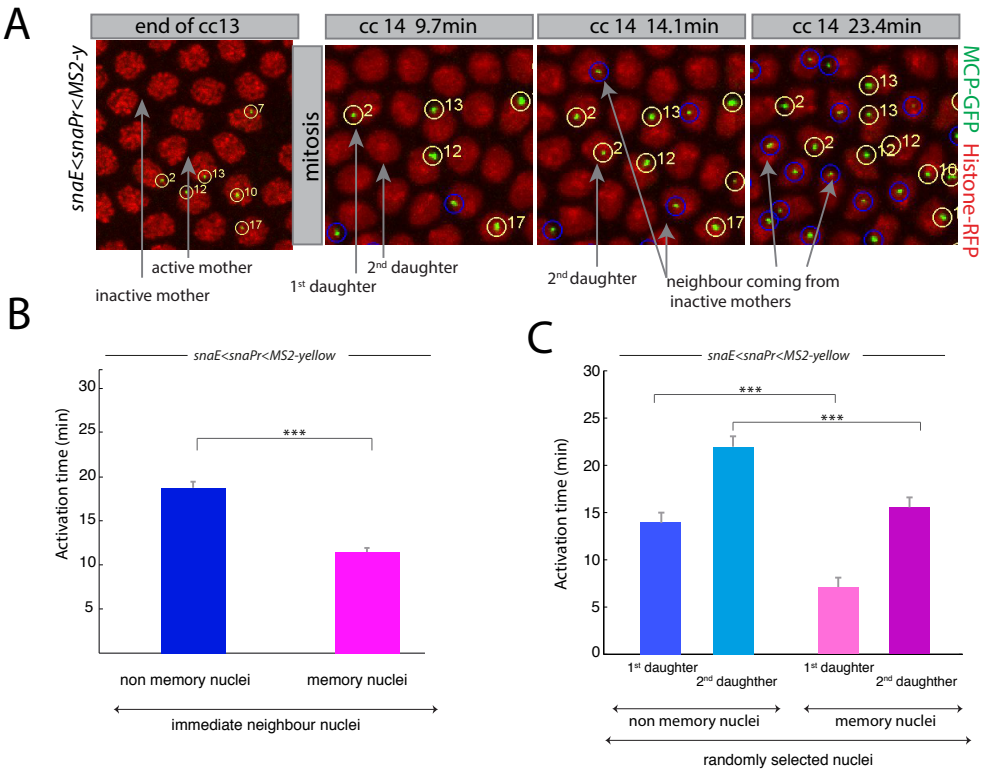

Figure 3.4: Transcriptional kinetic profiles of neighboring and sister nuclei.
(A) Zoomed in snapshots of live imaging embryos showing neighboring memory nuclei (yellow) and non memory nuclei (blue). (B) Mean activation time for non-memory nuclei (blue) and memory nuclei (magenta). (C) Mean activation time calculated for sister nuclei originated from non-memory (blue) and memory nuclei (magenta). Activation delay between spots of sister nuclei is present in both memory and non-memory nuclei. Three movies were analyzed for B and C (total of 750 nuclei) Error bars correspond to the standard error.

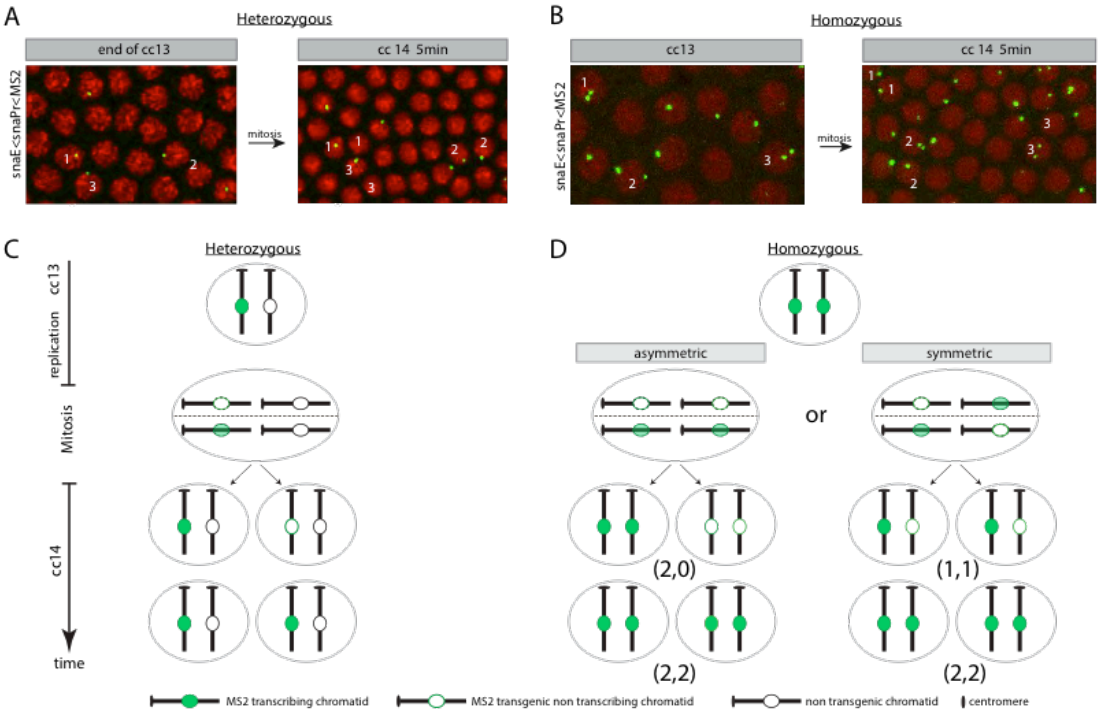

Figure 3.5: transcriptional memory behavior in homozygous embryos
(A-B) Zoomed in snapshots of live imaging embryos showing sister nuclei expression profiles in (A) heterozygous embryo and (B) homozygous embryo. Sister nuclei are labeled using Arabic numbers. (C) Schematic representation of the possible inheritance patterns in heterozygous and homozygous embryos, in case only one chromatid is active.

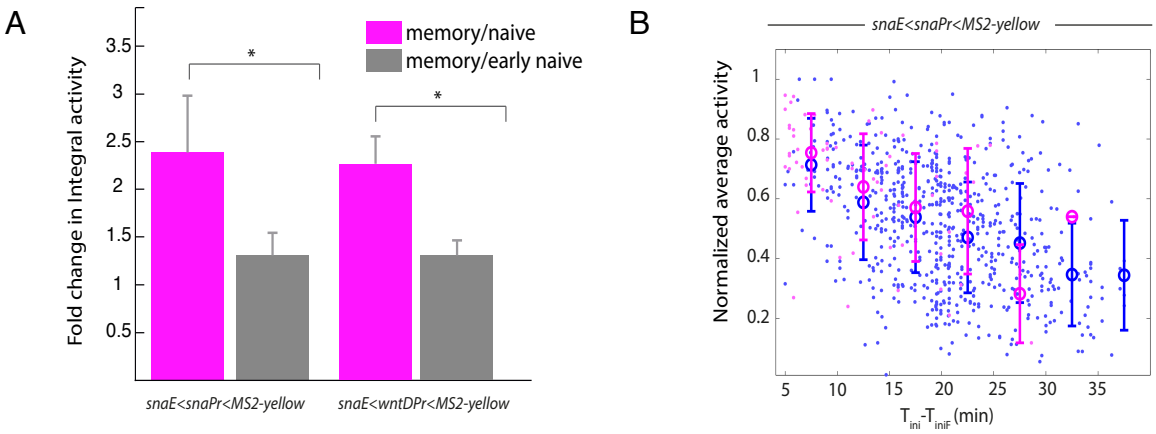

Figure 3.6: mRNA production of memory and non-memory nuclei
(A) Fold change in Integral activity. Integral activity corresponds to the total amount of mRNA production for a given nucleus for transgenes with either the snaPr or wntDPr. It is calculated adding the activity of the fluorescent spot across all the time frames. Mean integral activity of memory nuclei divided by the mean integral activity on non-memory nuclei (magenta). Mean integral activity of memory nuclei divided by the mean integral activity on non-memory nuclei that become active early. There is not a significant difference between memory and non-memory nuclei when they are activated at similar time points. (B) Scatterplot showing the integral activity of memory (magenta) and non-memory nuclei (blue) as function of time. The data points are extracted from three movies. Error bars correspond to the standard error.
.

Mitotic Silencing Facilitates Transcriptional Repression in Living *Drosophila* Embryos

4.1 Research aim

In this section I present the primary analysis on how repressors affect transcription in living early *Drosophila* embryos. We employ the MS2-MCP system to visualize in real-time the activity of the Snail repressor, which establishes the boundary between the presumptive mesoderm and the neurogenic ectoderm of early embryos. We propose that transcriptional repressors may prevent reactivation following mitotic silencing and further suggest that repressors exploit additional occurrences of transcriptional inactivity, such as the refractory periods between bursts. The computational analysis of this work was done in collaboration with Bomyi Lim, a postdoctoral student in the Levine lab, and with an undergraduate student Ghita Guessos in the lab of Thomas Gregor at Princeton University.

4.2 INTRODUCTION

Transcriptional repression is essential for the patterning of the body axes of the *Drosophila* embryo. Anterior-posterior patterning is initiated by the maternal Bicoid gradient, which produces sequential patterns of gap gene expression across the length of the early embryo (Driever & Nüsslein-Volhard 1988; Driever & Nüsslein-Volhard 1989; Struhl et al. 1989; Ochoa-Espinosa et al. 2005). The encoded gap proteins function as sequence-specific transcriptional repressors that subdivide the embryo into head, thoracic, and abdominal territories (Nüsslein-Volhard & Wieschaus 1980; Fowlkes et al. 2008; Surkova et al. 2008). They also delineate the borders of pair-rule stripes of gene expression underlying segmentation (Hiromi & Gehring 1987; Stanojevic et al. 1991; Small et al. 1991; Tsai & Gergen 1994). Similarly, the maternal Dorsal gradient leads to localized expression of several different transcriptional repressors across the dorsal-ventral axis of the early embryo (Ray et al. 1991; Casal & Leptin 1996; Stathopoulos et al. 2002; Stathopoulos & Levine 2005), including *snail* (*sna*) (Ashraf & Ip 2001; Hemavathy et al. 2004) and *brinker* (*brk*) (Jaźwińska et al. 1999; Zhang et al. 2001), which help delineate the limits of the mesoderm and ventral ectoderm, respectively (Kosman et al. 1991; Markstein et al. 2004).

The mechanisms underlying transcriptional repression, and hence the delineation of developmental boundaries, have been studied extensively. Several repression mechanisms have been documented, including competition between DNA binding proteins, “quenching” of activators bound to adjacent sites within target enhancers, or direct repression of the promoter (Levine & Manley 1989; Gray et al. 1994; Gray & Levine 1996a; Gray & Levine 1996b). The MS2-MCP method

permit the first opportunity to explore the temporal dynamics of these repression mechanisms in living embryos (Garcia et al. 2013; Lucas et al. 2013)

We examined the repression of two different tissue-specific enhancers, the 5' *brinker* (*brk*) enhancer and the intronic *short-gastrulation* (*sog*) enhancer. Both enhancers are activated by the maternal Dorsal gradient in ventral (presumptive mesoderm) and lateral (presumptive neurogenic ectoderm) regions of precellular embryos (Markstein et al. 2002; Stathopoulos et al. 2002a) . The Snail repressor binds to specific sites within each enhancer to exclude their activities within the mesoderm. We visualized the formation of this developmental boundary between mesoderm and neurogenic ectoderm in living embryos using the MS2-MCP detection method (e.g., Bothma et al. 2014; Bothma et al. 2015).

4.3 Materials and Methods

4.3.1 Cloning and transgenesis

The plasmids containing MS2 transgenes were generated using pbPHi, which contains the *yellow* reporter gene ((Venken et al. 2006; Perry et al. 2010) We amplified the enhancer (*sog* Distal, *sog* Intronic, *brk* 5') and promoter region (*sog*, *brk*) from *Drosophila* genomic DNA using primers listed in the table below. The enhancer was inserted into the pbPHi multiple cloning site using the NotI-XhoI restriction enzymes, while the promoter was inserted using XhoI-BamHI sites. 24 copies of the MS2 stem loops were enzymatically released from the 24XMS2SL-stable vector (Addgene; 31865) by digestion with BamHI and BglII restriction enzymes. It was subsequently inserted downstream of the promoter in the pbPHi vector containing an enhancer, promoter, and *yellow* reporter gene after being linearized with BamHI. All MS2 transgenes were integrated into the VK33 site of chromosome 3.

List of primers.

Primer name	Primer sequence
SogPrXhoI-F	ccctcgagTTGCTGCTGCATGTTGCGGCTG
SogPrBamHI-R	cgggatccATCGTATCGGATCGTATCG
SogShaR-Xho	atttgcggccgcGCCATCATTTAATCGAAGGACTGC
SogShaF-Not	ccctcgagTCAAAATCGCTTTCTTATGTC
SogIntF-Not	atttgcggccgc GTTGCCAATGCCATTGC
SogIntR-XhoI	cctcgagGCTTTATGGTCCATGGT
Brk-prim- NotI-F	atttgcggccgcCTCTGGCACAAACCCTAAATG
Brk-prim- XhoI-R	cctcgagGGGACAAGTGGCTCCCGCA
BrkPr XhoI-F	ccctcgagATTTCAGAGTGAACCGCAGTCG
BrkPr BamHI-R	cgggatccGCGTGCTGTTGCTTCTTCTGC

4.3.2 Fluorescent *In Situ* Hybridization and Immunostaining

2-4 hr *yellow;white* (*yw*) embryos were fixed as described by Kosman et al. (2004) Bothma et al. (2011) Hapten-tagged RNA probes were used for

hybridization, including the first intron of *yellow*, *brk* full-length cDNA and *sog* intronic sequence. Hybridized embryos were imaged with the Zeiss700 laser-scanning microscope in z-stacks through the nuclear layer at 0.5-μm intervals using a Plan-Apochromat 20x/0.8 air lens. Immunostained embryos were imaged on a Zeiss700 laser-scanning microscope in z stacks through the nuclear layer at 0.5-um intervals using a Plan-Apochromat 63x/1.4 air objective. The following primary antibodies were used for detection: sheep anti-digoxigenin and mouse anti-biotin (Roche Applied Sciences, Invitrogen). Both were labeled with Alexa dyes using Alexa Fluor 555-donkey-anti-sheep and Alexa Fluor 488 donkey-anti-mouse secondary antibodies (Invitrogen). Nuclei were stained with DAPI (Invitrogen). We used a mouse anti-Dorsal (74A - DSHB) antibody and a guinea-pig anti-Snail antibody (kindly provided by Dr. Wieschaus at Princeton University).

4.3.3 Live imaging sample preparation and data acquisition.

Virgin *yw*; Histone-RFP; MCP-NoNLS-GFP (Garcia et al. 2013) females were mated with homozygous males carrying *brk*>MS2, *sog*Intronic>MS2, or *sog*Distal>MS2 transgenes on Chromosome 3. Embryos were collected and mounted as described in Bothma et al. (2014)

Embryos were imaged on a Zeiss LSM 780 confocal microscope using a Plan-Apochromat 40x/1.4 N.A oil immersion objective. At each time point, a stack of 21 images separated by 0.5 μm was acquired, with the final time resolution of 20 sec. Images were taken at 512x512 pixels with a pinhole set to 115 μm diameter using bidirectional laser scanning. The same microscope settings (laser power, gain, etc) were used for or all of the datasets analyzed in this study.

4.3.4 Fly genetics

Increases in *snail* copy number were obtained using a fly strain homozygous for a BAC transgene (25 Kb) located on chromosome 3 (see Lagha et al. 2013). Males of this strain were mated with *yw*; Histone-RFP; MCP-NoNLS-GFP virgin females to obtain: *yw*; Histone-RFP/+ ; MCP-NoNLS-GFP/*sna*BAC. Virgin females were collected and mated with transgenic males carrying *sog*Intronic Enhancer>MS2 and embryos were imaged as described above. The progeny with the additional copy of the *snail* gene (50%) were retrospectively identified after imaging by PCR.

4.3.5 Live imaging Data analysis

Analysis of live images (mean fluorescent intensity of active nuclei and fraction of active nuclei) was performed as described by Garcia et al. (2013) and Bothma et al. (2014). The mesodermal and ectodermal regions were calculated using a heuristic algorithm that calculates the relative distance between nuclei in nc14 during gastrulation. In this way we were able to identify nuclei that are fated to undergo ventral furrow formation.

4.3.6 Lineage Tracking

A custom-made Matlab (Mathworks, 2015a) code was implemented to trace a nucleus splitting into two daughter nuclei during mitosis and to assign these daughter nuclei to the lineage of the mother nucleus. The lineage was manually corrected.

4.3.7 Analysis of homozygous embryos

A custom Matlab code was implemented to record the fluorescent intensity of the MS2 loci in a given nucleus. Each nucleus was segmented, and the maximum projected MS2 channel (488nm laser excitation) was converted into a binary image in a threshold-dependent manner. Each MS2 locus from a single nucleus was traced over time, and the fluorescent intensity of each locus was recorded. Nuclei with ambiguous separation of the two signals were excluded in this analysis. False-color images and movies shown in Fig.3 and Supplemental Movie S7-10 were generated by coloring the segmented nuclei with respect to the number of active alleles present in a given nucleus (green – both alleles active; yellow – one active allele; red – no active allele).

4.4 Results and discussion.

The enhancers tested in this study were derived from two different dorsal-ventral patterning genes, *brinker* (*brk*) and *short-gastrulation* (*sog*); both encode inhibitors of BMP signaling (Ashe & Levine 1999; Bray 1999; Campbell & Tomlinson 1999; Jaźwińska et al. 1999). The *brk* enhancer is located ~10 kb upstream of the transcription start site, while the *sog* enhancer is located within the first intron of the transcription unit, ~1.5 kb downstream of the start site (Fig. 4.1 A). Each enhancer was placed immediately upstream of its cognate promoter, and attached to a *yellow* reporter gene containing 24 MS2 stem loops within the 5' UTR. Nascent transcripts were visualized in living embryos using a maternally expressed MCP::GFP fusion protein (see Garcia et al., 2013; Fig. 4.1 B).

Both transgenes recapitulate the expression profiles of the endogenous genes, namely, they are activated throughout the presumptive mesoderm and neurogenic ectoderm and then repressed in the mesoderm. Earlier studies with fixed embryos indicated that these enhancers respond to different levels of the Snail repressor. The *brk* 5' enhancer appears to be more efficiently repressed by Snail as compared with the *sog* intronic enhancer. We examined both transgenes in living embryos to determine whether they exhibit distinctive repression dynamics.

4.4.1 *Brk* repression dynamics suggests a link to mitotic silencing

The *brk*>MS2 transgene exhibits an expression profile that is similar to that seen for the endogenous locus based on classical *in situ* hybridization methods (Fig.

4.1 C). The main difference is that the transgene produces a slightly narrower pattern due to the absence of the 3' "shadow" enhancer (Perry et al. 2010; Dunipace et al. 2013).

There is broad activation of the *brk*>MS2 transgene in both ventral and lateral regions during nc 10-13. *brk*>MS2 nascent transcripts are lost during the general silencing of transcription at each mitosis. Interestingly, upon reactivation of the transgene at the onset of nc14, we observe a striking absence of *de novo* transcription in the mesoderm (Fig. 4.2 A-B). Transcripts are restricted to the neurogenic ectoderm, suggesting that the mature *brk* expression pattern is established immediately after mitosis.

To better understand the dynamics of this repression, we conducted computational image analyses to partition the nuclei in either the mesoderm or ectoderm (see Fig. 4.3) and calculated the fraction of active nuclei in these regions throughout nc13 to nc14. We designate active nuclei as those exhibiting nascent RNA signals in at least one z-series (20 sec). We did not observe any significant variation in the number of active nuclei between the mesoderm and lateral ectoderm during nc13 (Fig. 4.2G). However, at the onset of nc14, ~90% of the active nuclei in the mesoderm were silenced while expression persisted in the lateral ectoderm (Fig. 4.2G).

To obtain more detailed information on the dynamics of repression in the ventral mesoderm, we quantified individual transcription foci since fluorescence intensities have been shown to scale with the number of Pol II complexes engaged in active transcription (Garcia et al. 2013; Bothma et al. 2014; Bothma et al. 2015). Quantitative imaging of the *brk*>MS2 transgene reveals that the ventral-most nuclei exhibit ~25% reduction in signal intensity during nc13 as compared with active nuclei in the lateral ectoderm (Fig. 4.2I, nc13). The majority of nuclei that display nascent transcripts at the onset of nc14 are located in the ectoderm, and the few active nuclei in the mesoderm show a dramatic reduction in signal intensity (Fig. 4.2I, nc14). This lingering expression is lost during the first 15 minutes of nc14. These observations suggest an unexpected link between mitosis and Snail-mediated repression. Snail begins to repress the *brk* 5' enhancer during nc13, and this repression is greatly reinforced at the onset of nc14 following mitosis.

4.4.2 *Sog* exhibits a more nuanced form of mitosis-associated repression

sog is regulated by two enhancers with overlapping activities, a distal enhancer located ~20 kb upstream of the *sog* promoter, and an intronic enhancer located ~1.5 kb downstream of the transcription start site (Hong, D. a Hendrix, et al. 2008; Perry et al. 2010). The distal 5' enhancer contains high-affinity Snail binding sites and exhibits similar repression dynamics as the *brk*>MS2 transgene following mitosis (Fig. 4.4). The intronic enhancer contains weak Snail binding sites and displays only modest repression in the ventral mesoderm (Fig. 4.2 D-F). Most nuclei are reactivated following mitotic silencing (Fig. 4.2 D-F and 1H),

but possess reduced signal intensities (Fig. 4.2J). These observations suggest that following mitosis *sog* expression is strongly attenuated in the mesoderm.

To determine whether the slower repression dynamics seen for the *sog*>MS2 transgene is due to low-affinity Snail repressor sites we examined its expression in transgenic embryos carrying three copies of the *snail* locus (Fig. 4.4). These embryos displayed significantly accelerated repression dynamics, with widespread failure to reactivate expression in the mesoderm following mitotic silencing (Fig. 4.4 A-C, G). These dynamics are similar to those seen for *brk*>MS2 in wild-type embryos and indicate that mitosis contributes to *sog* repression. In rare cases, Drosophila embryos can undergo to an extra nuclear division before gastrulation. This happens when the nuclear-cytoplasmic ratio falls below the 70% threshold of wild-type DNA as for example for haploid embryos (Lu et al., 2009). An extra division might be sufficient to observe *sog* repression after mitosis, even in the absence of extra Snail dosage. Indeed in such embryo we observe that *sog* behave similarly to wild-type embryos till mitosis nc13/nc14, where the nuclei are still active but significantly repressed. Upon the extra division, in nc15, all the nuclei in the mesoderm are silenced (Fig. 4.4 D-F, H). Altogether, these observations suggest that mitosis confers an advantage to Snail protein and thus facilitate repression. Because *sog* intronic enhancer present only weak Snail binding site, this mechanism is revealed only by increasing the repressor levels or by having an extra mitosis.

4.4.3 Allele by allele repression

The preceding analyses employed heterozygous embryos carrying a single copy of *brk* or *sog* transgenes. We next examined homozygous embryos to determine whether the two alleles of a locus display coordinated or uncoupled patterns of repression. *brk*>MS2 and *sog*>MS2 homozygotes initially exhibit broad patterns of expression in ventral and lateral regions, as seen for the corresponding heterozygotes. Roughly 25% of the ventral nuclei display gradual reductions in *brk*>MS2 expression from two to one to no active alleles during nc13 (Fig. 4.5B;). However, the other 75% express either one or both alleles at the end of nc13 (Fig. 4.5F). Following mitosis, most of the ventral nuclei fail to reactivate either allele during the onset of nc14 (Fig. 4.5 C,G). A small fraction exhibits transient activation of just a single allele. Most of these nuclei are located near the mesoderm/ectoderm boundary, suggesting limiting amounts of the Snail repressor (Fig. 4.5C; yellow nuclei; see below). By contrast, most of the nuclei in the lateral ectoderm reactivate both alleles at the onset of nc14 (Fig. 4.6).

There is no detectable ventral repression of either *sog*>MS2 allele during nc13 (Fig. 4.5D, H). Most of the daughter nuclei reactivate expression at the onset of nc14 following mitotic silencing. In the mesoderm, expression of 2 alleles persist in the nuclei upon mitosis and we observe a gradual reductions in expression from two to one to no active alleles over the course of the first 15 minutes of

nc14, similar to the repression pattern of *brk*>MS2 during nc 13 (Fig. 4.5 E, I). In the heterozygous *sog*>MS2 transgenic embryos we noticed that upon mitosis repression was observable at the fluorescent intensity level meaning that the transcript production was significantly impaired after mitosis. We wondered whether the expression levels were also affected in homozygous embryo. In this case we would expect that the alleles in the mesodermal nuclei are weaker that the alleles in the nuclei located in the ectoderm. When we calculated the total fluorescence intensity output for nuclei in the mesoderm versus the ectoderm, we observe a similar trend as in the heterozygous, suggesting that mitosis helped to lower *sog* expression (Fig. 4.7 A). Interestingly when we analyzed the alleles in the same nucleus, we noticed that in the ectoderm both alleles were characterized by comparable fluorescence intensity. On the contrary, a significant fraction of the nuclei in the mesoderm display monoallelic or asymmetric expression, whereby one allele has consistently stronger expression than the other beginning at the onset of nc14 (Fig. 4.7 B-C). These observations, along with the preceding analysis of the *brk*>MS2 transgene, suggest that each allele is independently repressed. Furthermore, the rapid silencing of *brk*>MS2 and the signal attenuation of one of the *sog*>MS2 alleles after mitosis reinforces the link between mitosis and Snail-mediated repression.

4.4.4 Lineage tracking suggests repression memory for *brk*>MS2

Lineage tracking was performed to measure individual nuclei expressing the *brk*>MS2 transgene before, during, and after mitosis. Nuclei were divided in three groups depending on the number of active alleles (2, 1 or 0) at the end of nc13, and their behaviors were monitored during the reactivation of gene expression at the onset of nc14 (Fig. 4.8A). Ventral nuclei that are off/off during nc13 never produce active daughters (on/on or on/off) in nc14 (Fig. 4.8A), consistent with the possibility of repression memory. In fact, most of the ventral nuclei that are on/on during nc13 nonetheless produce off/off daughters after mitosis (Fig. 4.8). This observation lends further evidence for a link between mitosis and Snail-mediated repression.

4.4.5 Proposed mechanism: Snail exploits intrinsic pauses in transcription

We have presented evidence that transcriptional repression is intimately linked to the cell cycle. Snail somehow exploits the general silencing of transcription that occurs during mitosis. Mitotic silencing offers an opportunity to reset the balance between transcriptional activators and repressors. It is possible that Snail out-competes the Dorsal activator during mitosis. Indeed, immunohistochemical localization assays suggest that the Snail repressor remains associated with the apical cytoplasm during mitosis (Fig. 4.9 A-C), while Dorsal becomes distributed throughout the cytoplasm (Fig. 4.9 A-C -F). This might give Snail “the jump” on Dorsal after the completion of mitosis. Snail appears poised to re-enter the

nucleus and rapidly find its target sites, while Dorsal may be slower to relocate from the cytoplasm to the nucleus.

We propose that Snail and other developmental repressors exploit natural pauses during transcription (summarized in Fig. 4.10). Mitotic silencing represents one such pause. Moreover, many genes exhibit transcriptional bursts during interphase, whereby gene expression is episodic and consists of cycles of intense and intermittent activity (e.g., Bothma et al. 2014). It is possible that repressors like Snail get the upper hand during the refractory periods between bursts. Indeed, we observe inhibition between successive bursts of *sog*>MS2 expression in the mesoderm following mitotic silencing. Many of these nuclei exhibit a single burst of expression before falling silent (Fig. 4.10), and we observe a similar trend in the repression of the *brk*>MS2 transgene (Fig.4.11). The Snail repressor may be more effective in maintaining the off state following a burst (or mitotic silencing) than inhibiting a gene at the peak of its activity. Mitotic silencing and transcriptional bursting might represent inherent mechanisms fostering dynamic repression of gene expression during development.

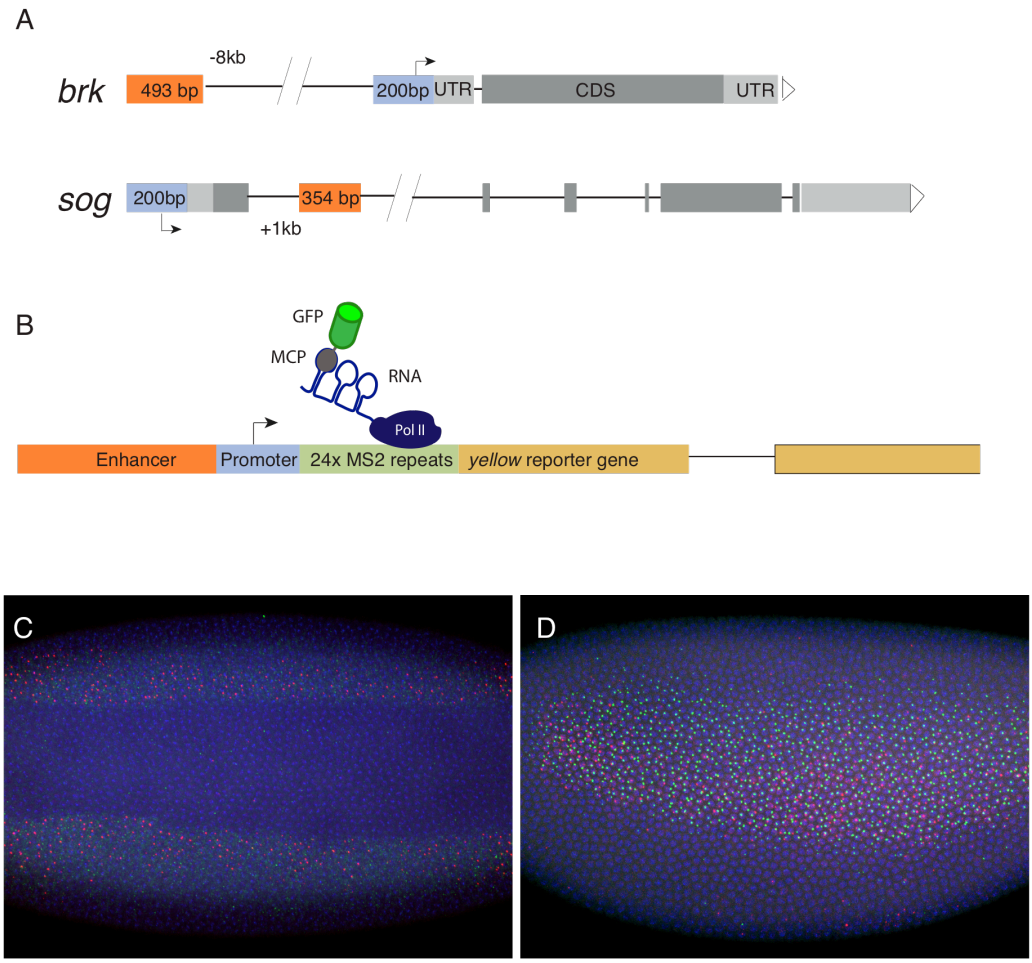

Fig. 4.1: Design of Transgenic plasmids.
(A) Genomic locus for the enhancer tested. 493bp of *brk* enhancer located 8 kb upstream the TSS and 354bp of *sog* intronic enhancer were chosen. (B) Schematic view of transgenic plasmids construction. For each construct, a minimal enhancer region was placed upstream of 24 repeats of an MS2 cassette followed by a *yellow* reporter gene. *sog*Enhancer-MS2 and brkEnhancer-MS2 constructs contain 200 bp of the *sog* and *brk* endogenous promoter, respectively. Upon transcriptional activation, the MS2 sequence forms a stemloop structure that is recognized by a MCP-GFP fusion protein, thus allowing visualization of nascent transcripts. (C-D) Fluorescent in situ hybridization of *Drosophila* embryos in nc 14 stained with a probe against the first intron of the *yellow* reporter gene (green) and a probe against *brk* full length cDNA (C - red) or a probe against the first intron of *sog* locus (D – red).

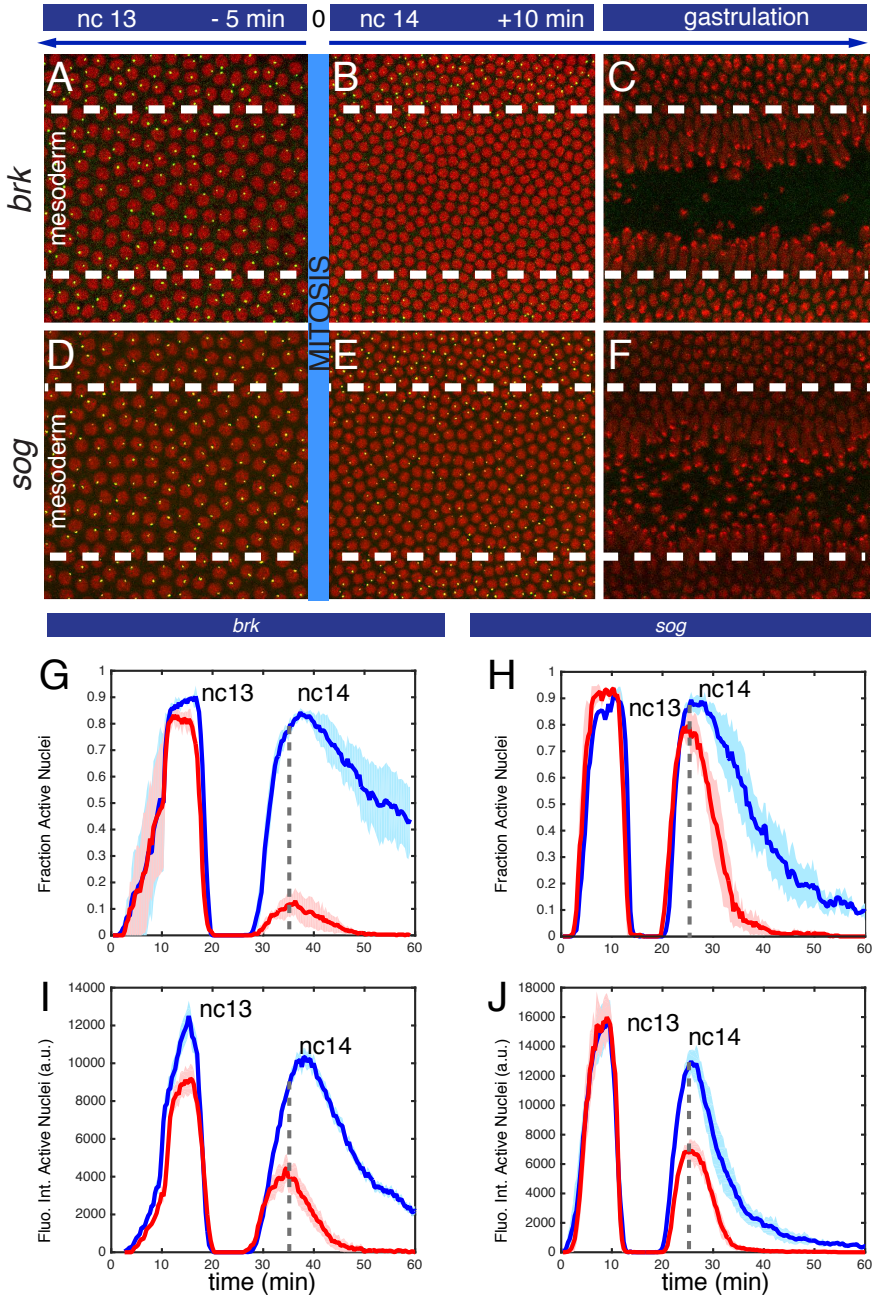

Fig. 4.2: Visualization of transcriptional repression in the mesoderm.
(A-F) Projected confocal stacks of a live embryo at three different time points during nc 13 and nc 14 expressing (A-C) *brk*>MS2 or (D-F) *sog*>MS2. Green dots correspond to nascent transcripts visualized with an MCP::GFP fusion protein. Histone-RFP was used to visualize the nuclei (red). The presumptive mesoderm encompasses the nuclei included between dashed lines and corresponds to the region that invaginates at the onset of gastrulation. (G-H) Fraction of nuclei that display nascent RNA signals during a 1-hr interval encompassing nc13, mitosis, and the first half of nc14. Ectoderm nuclei in blue and mesoderm nuclei in red. Mean values are represented by a continuous line. The shaded area corresponds to the standard error of the mean (SEM). (I-J) Mean fluorescence intensities in active nuclei, ectoderm (blue) and mesoderm (red). The shaded areas correspond to the SEM. Three separate movies for each transgene were averaged. The

times above each panel in A-C are scaled to the general silencing that occurs at mitosis (= time 0).

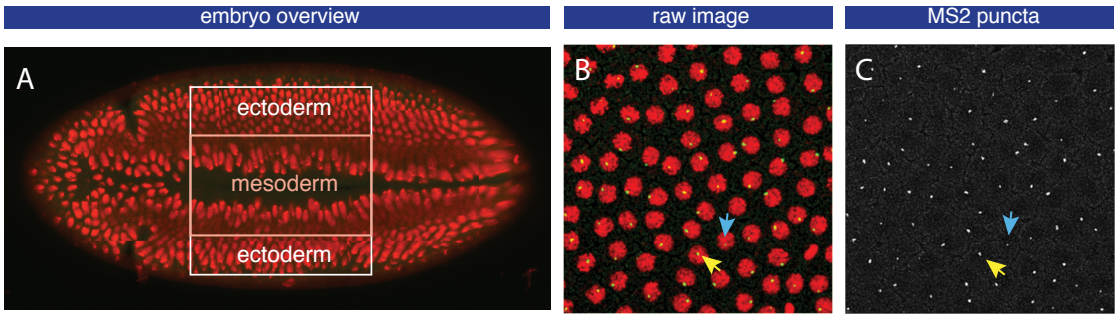

Fig. 4.3: Description of the image analysis
(A) Overview of a *Drosophila* embryo during the gastrulation stage: Tile array of a series of projected confocal stacks. The area imaged under the microscope is underlined in white; the morphology of the ventral furrow is used to define the mesodermal and the ectodermal area. (B) Projected confocal stack of a live *Drosophila* embryo. MCP-GFP is shown in green, His-RFP in red. (C) Projected confocal stack of a live *Drosophila* embryo, green channel only (displayed in gray): MCP-GFP in green. Yellow and blue arrows indicate weak and strong MCP-GFP signal, respectively

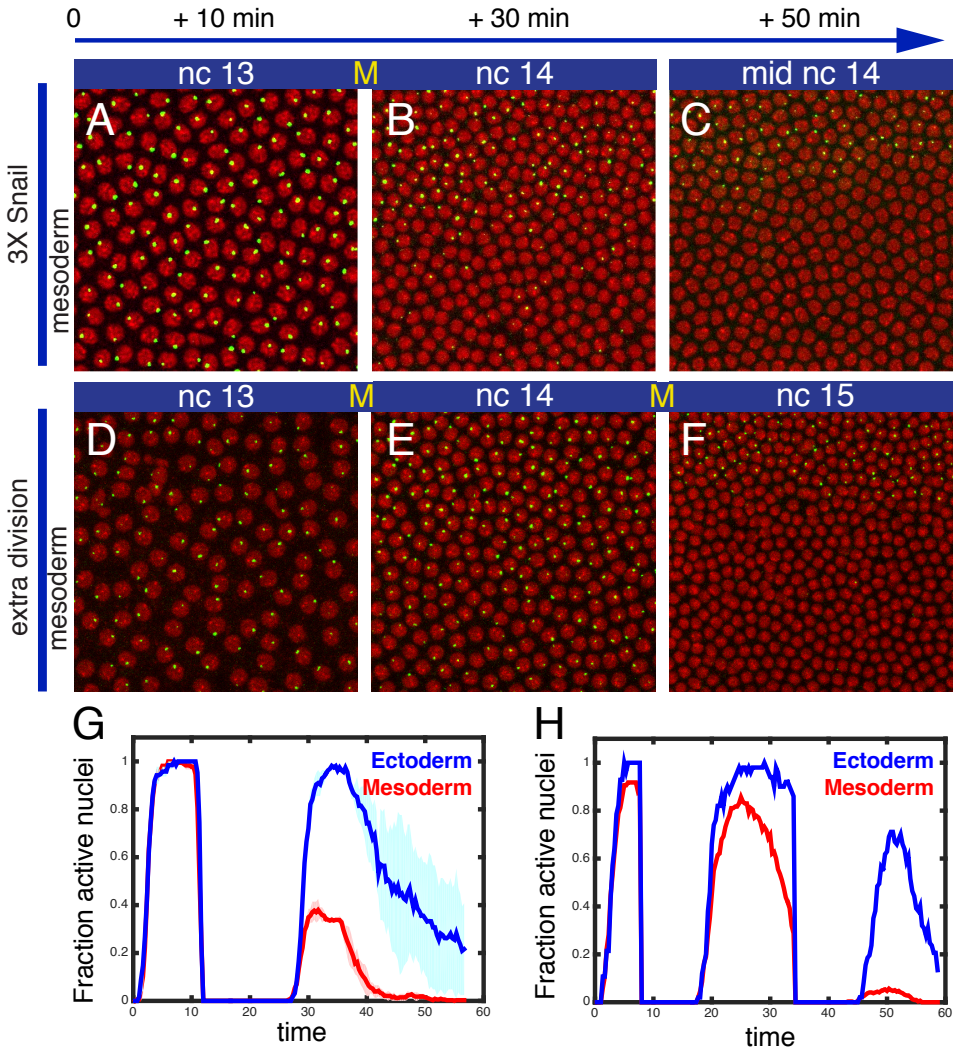

Fig. 4.4: two alternative way to accelerate repression of *sog*>MS2.
(A-C) Projected confocal stacks of a live embryo at three different time points during nc 13 and nc 14 expressing *sog*>MS2 are visualized with a MCP::GFP fusion protein (green) in embryo containing an extra copy of the Snail repressor. (D-F) Projected confocal stacks of a live embryo at three different time points during nc 13 and nc 15 expressing *sog*>MS2 are visualized with a MCP::GFP fusion protein (green). In figure F we can observe that the MS2 signal became OFF in the mesodermal region. (G-H) Fraction of nuclei that display nascent RNA signals during nc13, mitosis, nc14 for the embryo with 3 copies of Snail and during nc13, mitosis, nc14, mitosis, nc15 for the embryo undergoing an extra division. Ectoderm nuclei in blue and mesoderm nuclei in red. Mean values are represented by a continuous line. The shaded area corresponds to the standard error of the mean (SEM).Histone-RFP was used to visualize the nuclei (red). The times indicated above each panel indicate the temporal progression till the end of nc 13. Yellow M indicate the happening of mitosis.

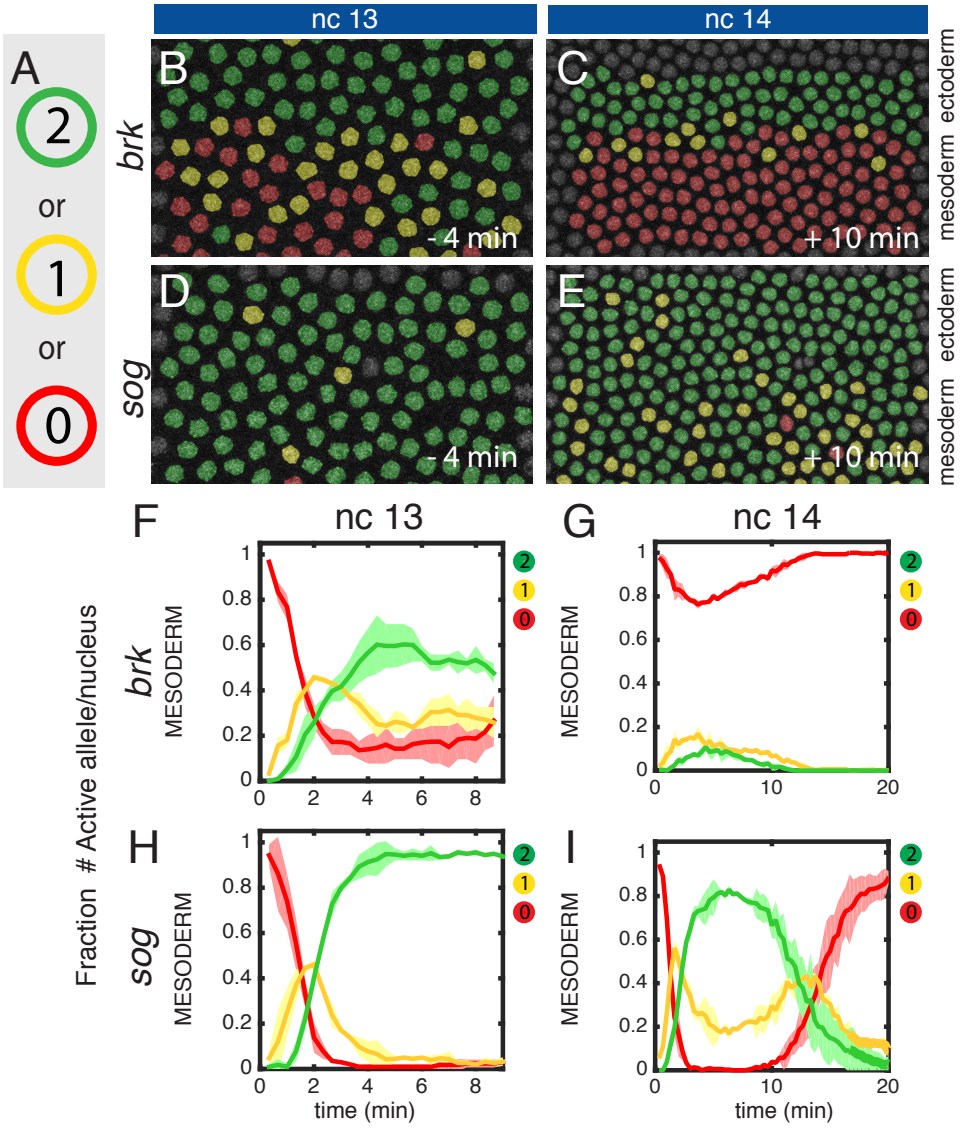

Fig.4.5: Transcriptional repression occurs one allele at a time.
(A) Schematic representation of transcriptional activity in homozygous embryos: 2 alleles active (green), 1 allele active (yellow), and no allele active (red). (B-E) False-colored maximum projected confocal stacks of a live embryo homozygous for either *brk*>MS2 (B-C) or *sog*>MS2 (D-E) at 2 different time points in nc 13 and nc 14 (times are scaled to mitosis). (F-I) Fraction of mesoderm nuclei exhibiting two (green), one (yellow) or no (red) active alleles during nc 13 (F,H) or nc 14 (G,I). The *brk*>MS2 transgene is shown in F,G and the *sog*>MS2 transgene in H,I. The shaded area corresponds to the standard error of the mean (SEM)

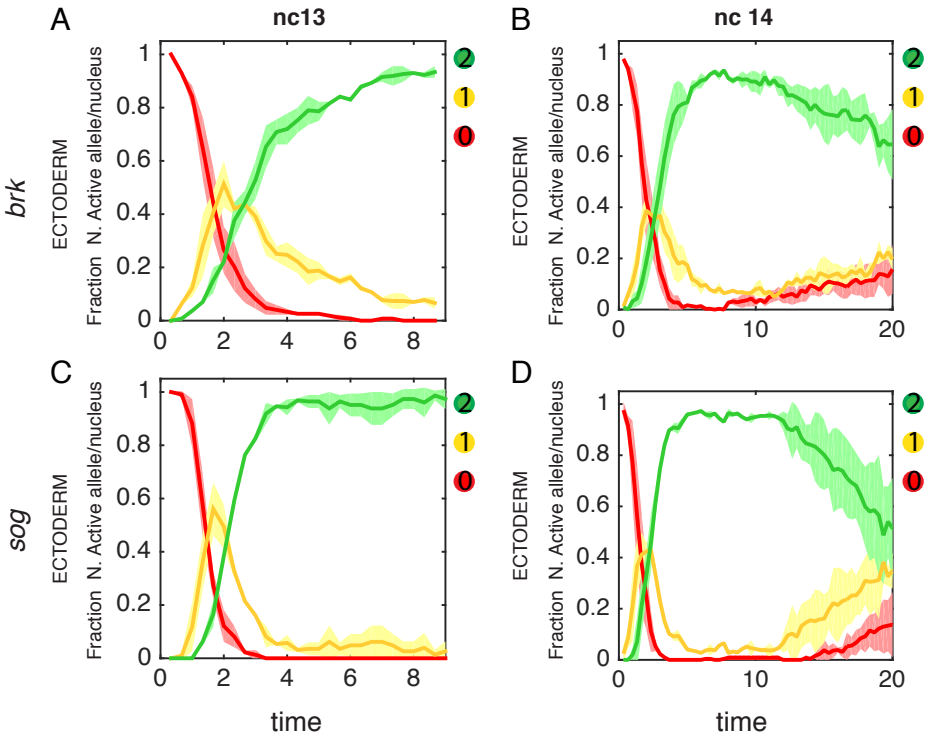

Fig. 4.6: Fraction of active allele over time in the ectodermal region
(A-B) Fraction of number of active alleles per nucleus over time for *brk* in the ectoderm during nc 13 and nc14 (C-D) Fraction of number of active alleles per nucleus over time for sog in the ectoderm during nc 13 and nc14. Red line corresponds to nuclei with 2 alleles ON, green 1 allele ON and blue indicate no transcription. The shaded area corresponds to the standard error of the mean (SEM).

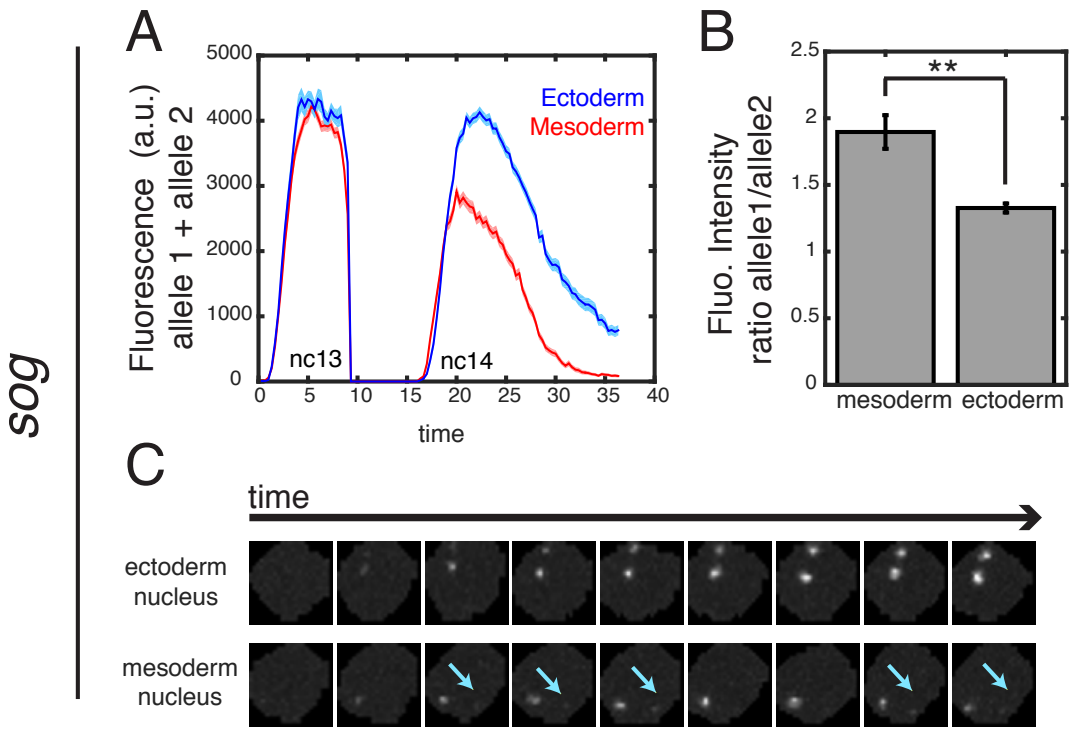

Fig.4.7: Differential expression of the two allele in mesodermal nuclei for *sog*>MS2
Mean fluorescence intensities (fluorescence allele 1 + fluorescence allele 2) in active nuclei, ectoderm (blue) and mesoderm (red). The shaded areas correspond to the SEM. (B) The *sog*>MS2 transgene exhibits asymmetric activities of homologous chromosomes. Ratio of transcriptional activity between the two alleles in ~30 nuclei in the mesoderm, ~30 nuclei in the ectoderm and (**) indicates p-value below 0.02. (C) Raw snapshots of a nucleus with two active alleles in the ectoderm and mesoderm for *sog*>MS2 transgene. Cyan arrows indicate the second (weak) allele in the nucleus.

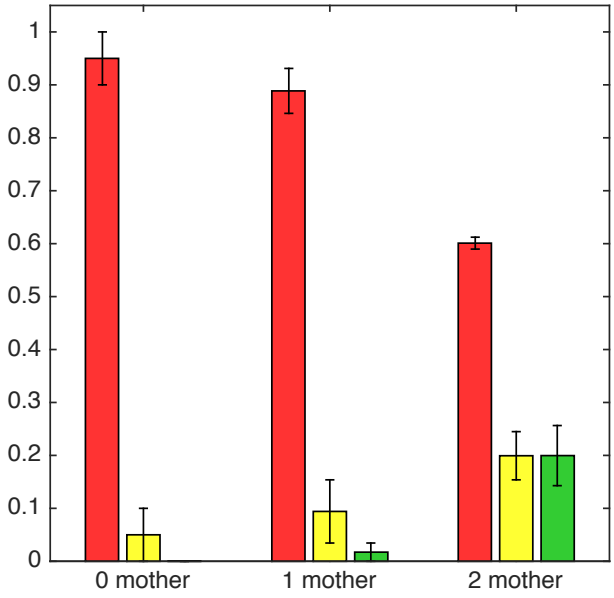

Fig. 4.8: Lineage tracking the nuclei in the mesoderm for *brk*>MS2.
Fraction of nuclei exhibiting 2 (green), 1 (yellow) or 0 (red) active alleles during nc 14 that originated from mother nuclei expressing neither allele (0 mother), one allele (1 mother), both alleles(2 mothers) at the end of nc13.

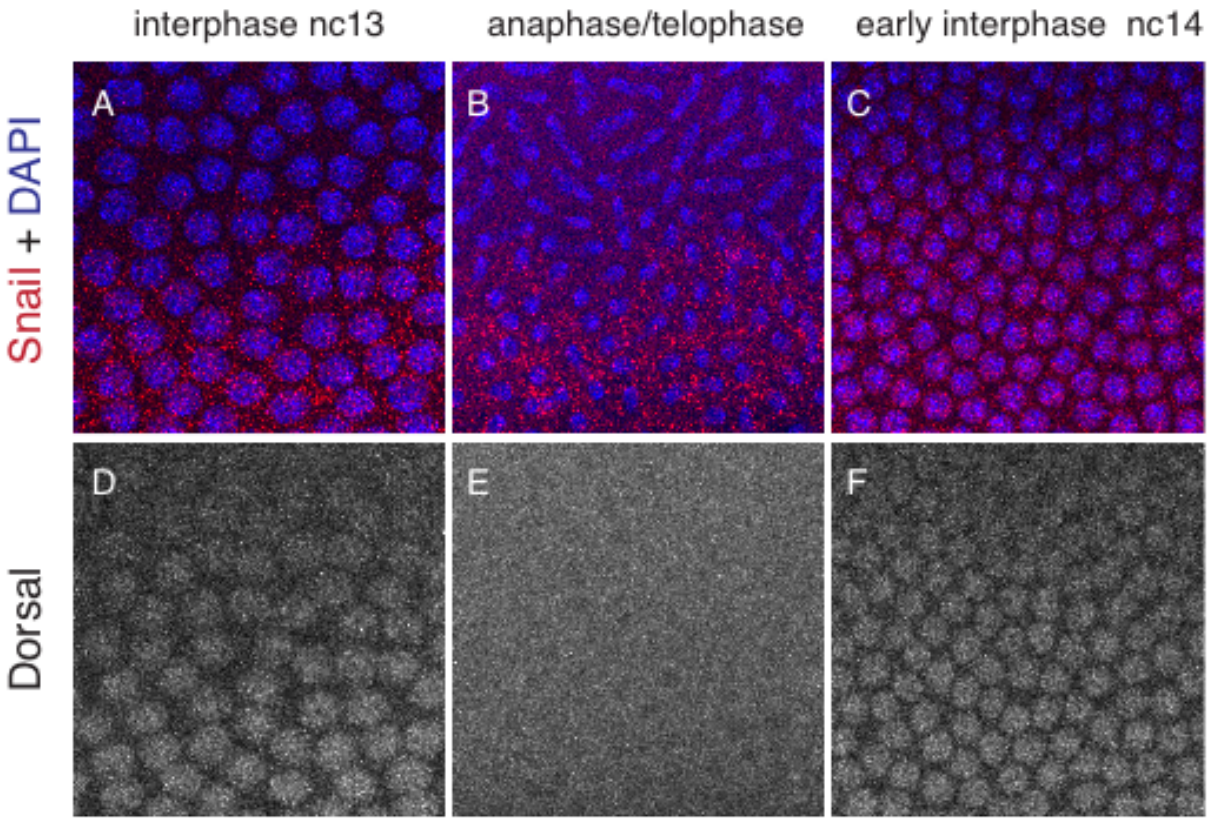

Fig. 4.9: Snail protein remains associates with the nucleoplasm during mitosis.
(A-F) Confocal Max projection of Drosophila fixed embryos stained with Snail (red) and Dorsal (gray) antibody during (A,D) interphase nc 13, (B,E) mitosis and (C,F) early interphase nc 14. Nuclei are stained with DAPI (blue).

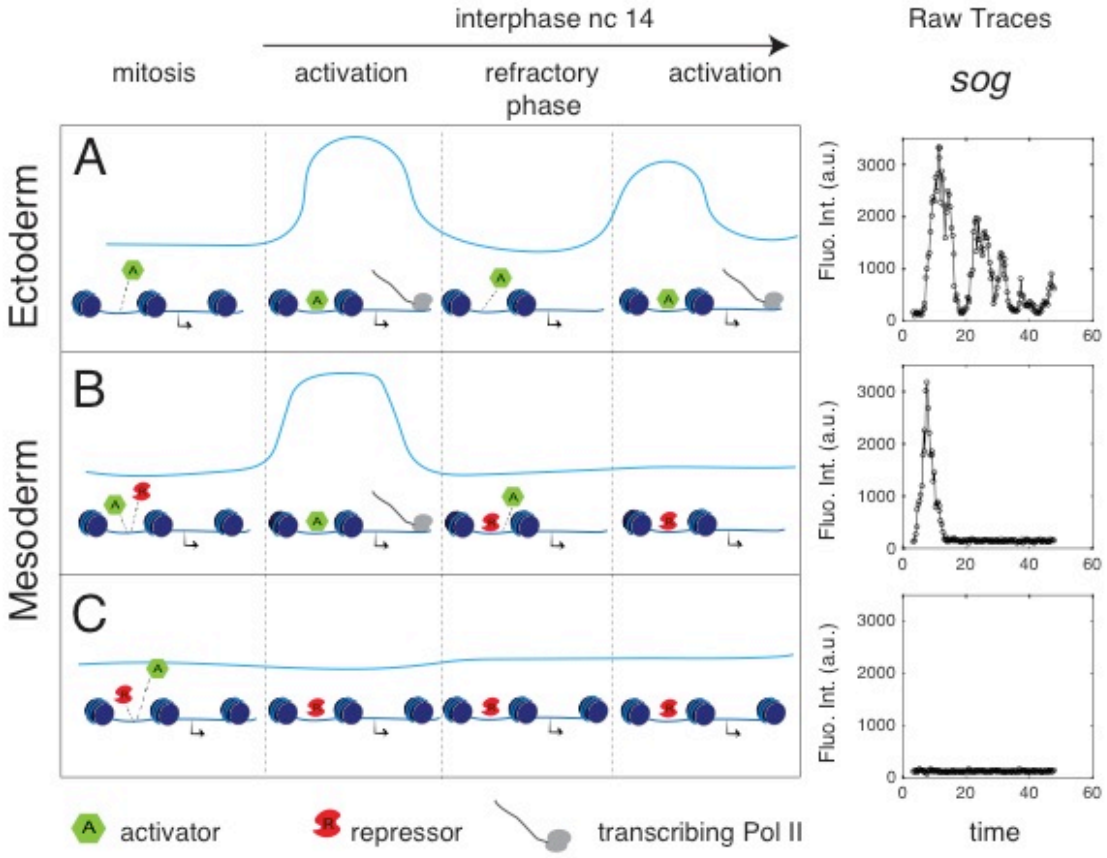

Fig. 4.10: Snail exploits intrinsic pauses in transcription.
Blue lines represent successive transcriptional bursts (levels, Y axis; time, X axis). Successive bursts are interrupted by mitotic silencing ("mitosis" above the diagram) or inherent refractory phases between bursts. The Snail repressor is absent in the ectoderm and there are successive bursts during nc 14 following mitotic silencing. In the mesoderm, the Snail repressor either prevents reactivation of transcription at the onset of nc 14 (C) or inhibits successive bursts during nc 14 (B). (D) Raw *sog*>MS2 fluorescent intensity traces for individual nuclei in the ectoderm (top panel), near the mesoderm/ectoderm boundary (middle panel), or within the mesoderm (bottom panel).

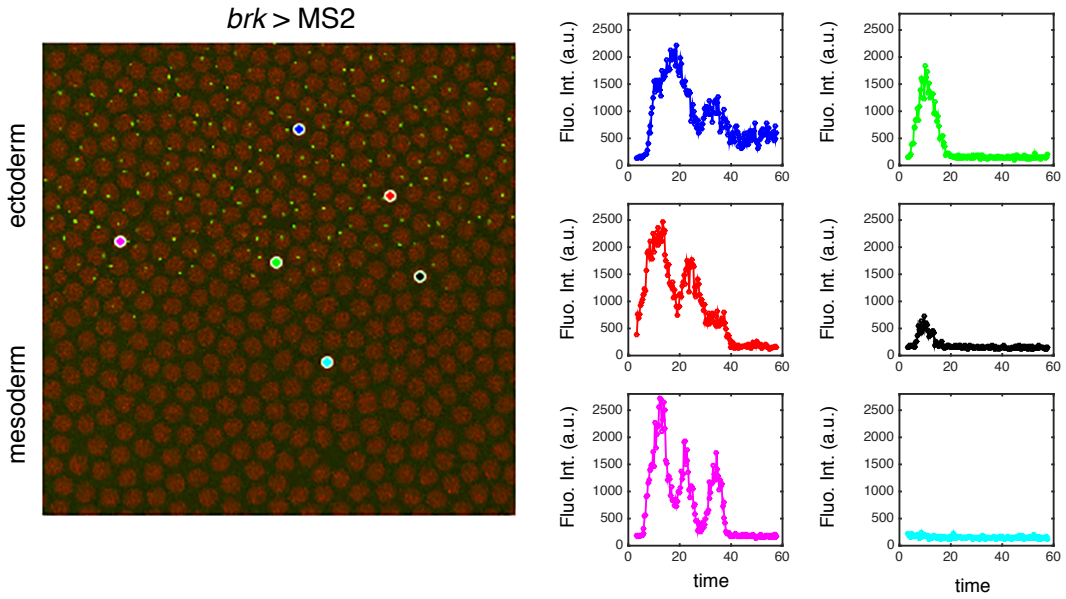

Fig. 4.11: Snail exploits intrinsic pauses in transcription.
Snapshot of brk>MS2 in nc14. We analyzed the fluorescent Intensity profile of multiple nuclei located in different DV axis. Single traces indicate that the number of transcriptional bursts decreseas going from the dorsal to ventral region.

Acknowledgements

Attending graduate school is like going to a roller coaster in an amusement park. It is exciting, frightening, intimidating, fun, heart-racing. It gives you adrenaline, and removes you breath. There are high points and low points. And yet, at any time, you can find at least another passenger that shares your emotions and enjoys the attractions with you. I cannot thank enough all the people that in a way or in another have shared this adventure with me.

First, I need to thank my friends Zenab and Ryan and their beautiful daughters, Samya and Kaya, for welcoming me in their house when I first arrived in Berkeley with the intent of revolutionizing my life. Without them I would have never embarked in this intercontinental, unexpected, long trip. In all these years, they have not only been my friends, but my adopting family.
I want to thank my friend “the dinosaur” Brateil. She was the first not familiar person to welcome me in Berkeley and become a truly beautiful friend (and a roommate).

Thank you to all the many other fantastic roommates I had the great pleasure to share this Berkeley unique experience: Chiara, Kevin, Lynn, Denia, Faiza, Sofia, Tibo, Ivan, my sweet, smart friend Lisa (a person that knows how to create beauty and makes everybody feel loved) and the “fun”tastic Alex that with his special way of thinking was able to make me always laugh – and yes Alex, we will be roommates once again when we will be too old to remember how crazy was living together. You are all very special.

Thank you to all my lab mates at UC Berkeley. Mike Perry, the fastest English speaking person I know. Mike with his deep curiosity and knowledge made me wish to perform my best. Mounia Lagha, a hard-core, pushy and full of determination scientist and, at the same time, a caring and close friend. You gave me passion, speed, accuracy and attentions to the controls. (Although, I may still need to work on my organizational skills). Jacques Bothma and Kevin Tsui, friends of many serious (and less serious) conversations. Jacques was a friend in all these years and introduced me to the fascinating world of imaging. And thank you to Valerie, Alistair, Eileen, Andy, Dominika, Ezzat, Blair, Phil, kasia, Laure, Thea, David and Sam.

Thank you to all my Berkeley and Princeton friends, a quite large group. You all were partners of many movies, gnocchi, pizze (or pizzas ☺), laughs, salsa dances, trips, coffee and so on. If Berkeley felt like home is also because of you.
Thank you to my Buddhist friends. You are one of the best encouraging group a person could ever wish for!
If in the past year I did not miss California too much, it is only because of my lab mates at Princeton University. A very special thanks goes to Bomyi Lim. You are

a smart, fun and hard-working woman. Thank you for giving me an exit strategy on the MAR project and being my friend. Thank you to Katrina and Emma with whom I shared this Berkeley-Princeton adaptation period and, on the way, laughed a lot. You are great friends and the best badminton teachers I met. And thank you to Takashi, Yuji, Will, Takeo, Ryoko, Nick, Kai, Philip, Laurence, Michal and Alex.
Thank you to my undergraduate students, both in Berkeley and Princeton. You challenged me and showed me how to be a mentor. Thank you for this special gift and your confidence in me.

Thank you to my MCB class. Especially to Cindy Wang, whose creativity goes far beyond science. It is always amazing to meet over a nice meal and discuss about music, design, cooking, photography, architecture, topographic fonts, trains, flies and so on.

Thank you to the Harland Lab. You are the best laboratory to be a neighbor of!

A huge thank you to my parents and sister Laura that did not allow me to give up when I wanted to quit. A Buddhist quote says: “the journey from Kamakura to Kyoto takes twelve days. If you travel for eleven but stop with only one day remaining, how can you admire the moon over the capital?” Hard times and setbacks should not defeat my curiosity and ability to succeed at the end. This is the spirit that my parents infused me with and I will be forever grateful for their teaching. I also thank them for having a wonderful light-hearted spirit.
I cannot thank enough my soon-to-be-husband Ekin. Your presence, even if on a distance, held me together. You kept alive my curiosity, lift my mood, shared my love for robots and challenged my Sudoku skills. Thank you for leading me through a world of infinite potential and infinite possibilities.

I want to thank all the members of the MCB graduate affair office, irreplaceable people always willing, to remind, help, suggest, comfort and guide. Thanks also to the administrative staff at the Lewis-Sigler Institute in Princeton, especially Marybeth Fedele, Barbara Chinery and Kara Dolinsky. You made me feel part of the Princeton team, even though I am still a Cal bear.
Thank you to Amanda Amodeo for co-organizing with me the Ichan Think and drink lecture series. It was a great fun.

Thank you to Thomas Gregor, Teresa Ferraro and Hernan Garcia for being valuable collaborators.

I want to thank my Qualification exams committee members: Don Rio, John Gerhart, Craig, Miller and Lewis Feldman. You questioned me with constructive criticism and made me feel accepted as a growing scientist.

Prof. Feldman and Prof. Rio continued to follow me as member of my thesis committee together with Nipam Patel. Their advices were very helpful to succeed and remain on track. Thank you.

Lastly I cannot express enough my gratitude towards my advisor Mike Levine.
The first time I met with Mike, I fell in a “scientific love” after five minutes. Mike’s ability to see the big picture without losing the attention for details, his unique way to connect the dots and communicate science in an accessible way (it resembles more a fun comedy than a lecture); his almost neurotic, but genuine, desire to discover more, see more, understand more and of course have more DATA, made my past 6 years with him twisting between great excitements and desperations. There are still a lot of things I wish I could learn from him and I am certain I will miss our intensely long lab meetings, the scary progress reports (timely reminders of lack of DATA), the nickname(s) and writing a paper together.
If I started as a timid stubborn student and now I am more grounded and confident is because Mike, through challenges, gave me a chance.
Thank you for giving me the chance to be a Cinderella.

Bibliography

Alberts, B. et al., 2002. Drosophila and the Molecular Genetics of Pattern Formation: Genesis of the Body Plan.

Arnosti, D.N. et al., 1996. The eve stripe 2 enhancer employs multiple modes of transcriptional synergy. *Development (Cambridge, England)*, 122(1), pp.205–14.

Ashe, H.L. & Levine, M., 1999. Local inhibition and long-range enhancement of Dpp signal transduction by Sog. *Nature*, 398(6726), pp.427–31.

Ashraf, S.I. & Ip, Y.T., 2001. The Snail protein family regulates neuroblast expression of inscuteable and string, genes involved in asymmetry and cell division in Drosophila. *Development*, 128(23), pp.4757–4767.

Bertrand, E. et al., 1998. Localization of ASH1 mRNA particles in living yeast. *Molecular cell*, 2(4), pp.437–45.

Boettiger, A.N. & Levine, M., 2013. Rapid transcription fosters coordinate snail expression in the Drosophila embryo. *Cell reports*, 3(1), pp.8–15.

Boettiger, A.N. & Levine, M., 2009. Synchronous and stochastic patterns of gene activation in the Drosophila embryo. *Science (New York, N.Y.)*, 325(5939), pp.471–3.

ten Bosch, J.R., Benavides, J.A. & Cline, T.W., 2006. The TAGteam DNA motif controls the timing of Drosophila pre-blastoderm transcription. *Development (Cambridge, England)*, 133(10), pp.1967–77.

Bothma, J.P. et al., 2014. Dynamic regulation of eve stripe 2 expression reveals transcriptional bursts in living Drosophila embryos. *Proceedings of the National Academy of Sciences of the United States of America*, 111(29), pp.10598–603.

Bothma, J.P. et al., 2015. Enhancer additivity and non-additivity are determined by enhancer strength in the Drosophila embryo. *eLife*, 4.

Bothma, J.P., Magliocco, J. & Levine, M., 2011. The snail repressor inhibits release, not elongation, of paused Pol II in the Drosophila embryo. *Current biology : CB*, 21(18), pp.1571–7.

Bray, S., 1999. DPP on the brinker. *Trends in Genetics*, 15(4), p.140.

Buxbaum, A.R., Haimovich, G. & Singer, R.H., 2014. In the right place at the right time: visualizing and understanding mRNA localization. *Nature Reviews Molecular Cell Biology*, 16(2), pp.95–109.

Campbell, G. & Tomlinson, A., 1999. Transducing the Dpp Morphogen Gradient in the Wing of Drosophila. *Cell*, 96(4), pp.553–562.

Casal, J. & Leptin, M., 1996. Identification of novel genes in Drosophila reveals the complex regulation of early gene activity in the mesoderm. *Proceedings of the National Academy of Sciences of the United States of America*, 93(19), pp.10327–32.

Chubb, J.R. et al., 2006. Transcriptional pulsing of a developmental gene. *Current biology : CB*, 16(10), pp.1018–25.

Coppey, M. et al., 2007. Modeling the bicoid gradient: diffusion and reversible nuclear trapping of a stable protein. *Developmental biology*, 312(2), pp.623–30.

Coppey, M. et al., 2008. Nuclear trapping shapes the terminal gradient in the Drosophila embryo. *Current biology : CB*, 18(12), pp.915–9.

Dar, R.D. et al., 2012. Transcriptional burst frequency and burst size are equally modulated across the human genome. *Proceedings of the National Academy of Sciences of the United States of America*, 109(43), pp.17454–9.

Darzacq, X. et al., 2009. Imaging transcription in living cells. *Annual review of biophysics*, 38, pp.173–96.

Driever, W. & Nüsslein-Volhard, C., 1988. A gradient of bicoid protein in Drosophila embryos. *Cell*, 54(1), pp.83–93.

Driever, W. & Nüsslein-Volhard, C., 1989. The bicoid protein is a positive regulator of hunchback transcription in the early Drosophila embryo. *Nature*, 337(6203), pp.138–143. xt t

Dunipace, L. et al., 2013. Autoregulatory feedback controls sequential action of cis-regulatory modules at the brinker locus. *Developmental cell*, 26(5), pp.536–43.

Eliscovich, C. et al., 2013. mRNA on the move: the road to its biological destiny. *The Journal of biological chemistry*, 288(28), pp.20361–8.

Ferraro, T., et al., 2016. Transcriptional Memory in the Drosophila Embryo. *Current Biology : CB*, *26*(2), 212–8. http://doi.org/10.1016/j.cub.2015.11.058

Ferraro, T. et al., 2016. New methods to image transcription in living fly embryos: the insights so far, and the prospects. *Wiley interdisciplinary reviews. Developmental biology*, 5(3), pp.296–310.

Fowlkes, C.C. et al., 2008. A quantitative spatiotemporal atlas of gene expression in the Drosophila blastoderm. *Cell*, 133(2), pp.364–74.

Francis, N.J. & Kingston, R.E., 2001. Mechanisms of transcriptional memory. *Nature reviews. Molecular cell biology*, 2(6), pp.409–21.

Frasch, M. & Levine, M., 1987. Complementary patterns of even-skipped and fushi tarazu expression involve their differential regulation by a common set of segmentation genes in Drosophila. *Genes & development*, 1(9), pp.981–95.

Garcia, H.G. et al., 2013. Quantitative Imaging of Transcription in Living Drosophila Embryos Links Polymerase Activity to Patterning. *Current Biology*, 23(21), pp.2140–2145.

Gilmourt, D.S. & Lis, J.T., 2009. RNA Polymerase. , 6(11), pp.3984–3989.

Goto, T., Macdonald, P. & Maniatis, T., 1989. Early and late periodic patterns of even skipped expression are controlled by distinct regulatory elements that respond to different spatial cues. *Cell*, 57(3), pp.413–22.

Gray, S. & Levine, M., 1996a. Short-range transcriptional repressors mediate both quenching and direct repression within complex loci in Drosophila. *Genes & development*, 10(6), pp.700–10.

Gray, S. & Levine, M., 1996b. Transcriptional repression in development. *Current opinion in cell biology*, 8(3), pp.358–64.

Gray, S., Szymanski, P. & Levine, M., 1994. Short-range repression permits multiple enhancers to function autonomously within a complex promoter. *Genes & development*, 8(15), pp.1829–38.

Harding, K. et al., 1989. Autoregulatory and gap gene response elements of the even-skipped promoter of Drosophila. *The EMBO journal*, 8(4), pp.1205–12.

Hemavathy, K. et al., 2004. The repressor function of snail is required for Drosophila gastrulation and is not replaceable by Escargot or Worniu. *Developmental biology*, 269(2), pp.411–20.

Hiromi, Y. & Gehring, W.J., 1987. Regulation and function of the Drosophila segmentation gene fushi tarazu. *Cell*, 50(6), pp.963–74.

Hocine, S. et al., 2013. Single-molecule analysis of gene expression using two-color RNA labeling in live yeast. *Nature methods*, 10(2), pp.119–21.

Hong, J.-W., Hendrix, D.A., et al., 2008. How the Dorsal gradient works: insights from postgenome technologies. *Proceedings of the National Academy of Sciences of the United States of America*, 105(51), pp.20072–6.

Hong, J.-W., Hendrix, D. a & Levine, M.S., 2008. Shadow enhancers as a source of evolutionary novelty. *Science (New York, N.Y.)*, 321(5894), p.1314.

Hoskins, R.A. et al., 2011. Genome-wide analysis of promoter architecture in Drosophila melanogaster. *Genome research*, 21(2), pp.182–92.

Ip, Y.T. et al., 1992. The dorsal gradient morphogen regulates stripes of rhomboid expression in the presumptive neuroectoderm of the Drosophila embryo. *Genes & development*, 6(9), pp.1728–39.

Jacob, F. & Monod, J., 1961. Genetic regulatory mechanisms in the synthesis of proteins. *Journal of Molecular Biology*, 3(3), pp.318–356.

Jaźwińska, A. et al., 1999. The Drosophila gene brinker reveals a novel mechanism of Dpp target gene regulation. *Cell*, 96(4), pp.563–73.

Jenkins, D.J., Finkenstädt, B. & Rand, D.A., 2013. A temporal switch model for estimating transcriptional activity in gene expression. *Bioinformatics (Oxford, England)*, 29(9), pp.1158–65.

Jiang, J., Hoey, T. & Levine, M., 1991. Autoregulation of a segmentation gene in Drosophila: combinatorial interaction of the even-skipped homeo box protein with a distal enhancer element. *Genes & development*, 5(2), pp.265–77.

Kosman, D. et al., 1991. Establishment of the mesoderm-neuroectoderm boundary in the Drosophila embryo. *Science (New York, N.Y.)*, 254(5028), pp.118–22.

Kosman, D. et al., 2004. Multiplex detection of RNA expression in Drosophila embryos. *Science (New York, N.Y.)*, 305(5685), p.846.

Kvon, E.Z., 2015. Using transgenic reporter assays to functionally characterize enhancers in animals. *Genomics*, 106(3), pp.185–92.

Kwak, H. & Lis, J.T., 2013. Control of Transcriptional Elongation., (September), pp.501–526.

Lagha, M. et al., 2013. Paused Pol II coordinates tissue morphogenesis in the Drosophila embryo. *Cell*, 153(5), pp.976–87.

Larkin, J.D. et al., 2013. Space exploration by the promoter of a long human gene during one transcription cycle. *Nucleic acids research*, 41(4), pp.2216–27.

Levine, M., 2010. Transcriptional Enhancers in Animal Development and Evolution. *Current Biology*, 20(17), pp.R754–R763.

Levine, M. & Davidson, E.H., 2005. Gene regulatory networks for development. *Proceedings of the National Academy of Sciences of the United States of America*, 102(14), pp.4936–42.

Levine, M. & Manley, J.L., 1989. Transcriptional repression of eukaryotic promoters. *Cell*, 59(3), pp.405–8.

Lewis, E.B., 1978. A gene complex controlling segmentation in Drosophila. *Nature*, 276(5688), pp.565–570.

Lionnet, T. & Singer, R.H., 2012. Transcription goes digital. *EMBO reports*, 13(4), pp.313–21.

Lipshitz, H.D., 2009. Follow the mRNA: a new model for Bicoid gradient formation. *Nature reviews. Molecular cell biology*, 10(8), pp.509–12.

Lu, X. et al., 2009. Coupling of zygotic transcription to mitotic control at the

Drosophila mid-blastula transition. *Development (Cambridge, England)*, 136(12), pp.2101–10.

Lucas, T. et al., 2013. Live imaging of bicoid-dependent transcription in Drosophila embryos. *Current biology : CB*, 23(21), pp.2135–9.

Lyon, M.F., 1961. Gene Action in the X-chromosome of the Mouse (Mus musculus L.). *Nature*, 190(4773), pp.372–373.

Macdonald, P.M., Ingham, P. & Struhl, G., 1986. Isolation, structure, and expression of even-skipped: a second pair-rule gene of Drosophila containing a homeo box. *Cell*, 47(5), pp.721–34.

Markstein, M. et al., 2004. A regulatory code for neurogenic gene expression in the Drosophila embryo. *Development (Cambridge, England)*, 131(10), pp.2387–94. Available at: http://www.ncbi.nlm.nih.gov/pubmed/15128669 [Accessed January 26, 2016].

Markstein, M. et al., 2002. Genome-wide analysis of clustered Dorsal binding sites identifies putative target genes in the Drosophila embryo. *Proceedings of the National Academy of Sciences of the United States of America*, 99(2), pp.763–8.

Misteli, T., 2008. Physiological importance of RNA and protein mobility in the cell nucleus. *Histochemistry and cell biology*, 129(1), pp.5–11.

Muramoto, T. et al., 2010. Methylation of H3K4 Is required for inheritance of active transcriptional states. *Current biology : CB*, 20(5), pp.397–406.

Muse, G.W. et al., 2007. RNA polymerase is poised for activation across the genome. , 39(12), pp.1507–1511.

Nien, C.-Y. et al., 2011. Temporal coordination of gene networks by Zelda in the early Drosophila embryo. *PLoS genetics*, 7(10), p.e1002339.

Nüsslein-Volhard, C., Kluding, H. & Jürgens, G., 1985. Genes affecting the segmental subdivision of the Drosophila embryo. *Cold Spring Harbor symposia on quantitative biology*, 50, pp.145–54.

Nüsslein-Volhard, C. & Wieschaus, E., 1980. Mutations affecting segment number and polarity in Drosophila. *Nature*, 287(5785), pp.795–801.

Ochoa-Espinosa, A. et al., 2005. The role of binding site cluster strength in Bicoid-dependent patterning in Drosophila. *Proceedings of the National Academy of Sciences of the United States of America*, 102(14), pp.4960–5.

Park, H.Y., Buxbaum, A.R. & Singer, R.H., 2010. Single mRNA tracking in live cells. *Methods in enzymology*, 472, pp.387–406.

Perry, M.W. et al., 2010. Shadow enhancers foster robustness of Drosophila gastrulation. *Current biology : CB*, 20(17), pp.1562–7.

Perry, M.W., Boettiger, A.N. & Levine, M., 2011. Multiple enhancers ensure precision of gap gene-expression patterns in the Drosophila embryo. *PNAS*, 108(33).

Phair, R.D. & Misteli, T., 2001. Kinetic modelling approaches to in vivo imaging. *Nature reviews. Molecular cell biology*, 2(12), pp.898–907.

Ptashne, M., 2008. Transcription: a mechanism for short-term memory. *Current biology : CB*, 18(1), pp.R25–7.

Rafalska-Metcalf, I.U. et al., 2010. Single cell analysis of transcriptional activation dynamics. *PloS one*, 5(4), p.e10272.

Rafalska-Metcalf, I.U. & Janicki, S.M., 2013. Preparation of cell lines for single-cell analysis of transcriptional activation dynamics. *Methods in molecular biology (Clifton, N.J.)*, 977, pp.249–58.

Rajala, T. et al., 2010. Effects of transcriptional pausing on gene expression dynamics. *PLoS computational biology*, 6(3), p.e1000704.

Ray, R.P. et al., 1991. The control of cell fate along the dorsal-ventral axis of the Drosophila embryo. *Development (Cambridge, England)*, 113(1), pp.35–54.

Rushlow, C.A. & Shvartsman, S.Y., 2012. Temporal dynamics, spatial range, and transcriptional interpretation of the Dorsal morphogen gradient. *Current opinion in genetics & development*, 22(6), pp.542–6.

Saad, H. et al., 2014. DNA dynamics during early double-strand break processing revealed by non-intrusive imaging of living cells. *PLoS genetics*, 10(3), p.e1004187.

Sadasivam, D.A. & Huang, D.-H., 2016. Maintenance of Tissue Pluripotency by Epigenetic Factors Acting at Multiple Levels. *PLoS genetics*, 12(2), p.e1005897.

Schaffner, W., 2015. Enhancers, enhancers - from their discovery to today's universe of transcription enhancers. *Biological chemistry*, 396(4), pp.311–27.

Singh, A. et al., 2010. Transcriptional Bursting from the HIV-1 Promoter Is a Significant Source of Stochastic Noise in HIV-1 Gene Expression. *Biophysj*, 98(8), pp.L32–L34.

Small, S. et al., 1991. Transcriptional regulation of a pair-rule stripe in Drosophila. *Genes & development*, 5(5), pp.827–39.

Small, S., Blair, A. & Levine, M., 1992. Regulation of even-skipped stripe 2 in the Drosophila embryo. *The EMBO journal*, 11(11), pp.4047–57.

Stanojević, D., Hoey, T. & Levine, M., 1989. Sequence-specific DNA-binding activities of the gap proteins encoded by hunchback and Krüppel in Drosophila. *Nature*, 341(6240), pp.331–5.

Stanojevic, D., Small, S. & Levine, M., 1991. Regulation of a segmentation stripe by overlapping activators and repressors in the Drosophila embryo. *Science (New York, N.Y.)*, 254(5036), pp.1385–7.

Stathopoulos, A. et al., 2002. Whole-Genome Analysis of Dorsal-Ventral Patterning in the Drosophila Embryo. *Cell*, 111(5), pp.687–701.

Stathopoulos, A. & Levine, M., 2005. Genomic regulatory networks and animal development. *Developmental cell*, 9(4), pp.449–62.

Struhl, G., Struhl, K. & Macdonald, P.M., 1989. The gradient morphogen bicoid is a concentration-dependent transcriptional activator. *Cell*, 57(7), pp.1259–1273.

Surkova, S. et al., 2008. Characterization of the Drosophila segment determination morphome. *Developmental biology*, 313(2), pp.844–62.

Suter, D.M. et al., 2011. Mammalian genes are transcribed with widely different bursting kinetics. *Science (New York, N.Y.)*, 332(6028), pp.472–4.

Tsai, C. & Gergen, J., 1994. Gap gene properties of the pair-rule gene runt during Drosophila segmentation. *Development*, 120(6), pp.1671–1683.

Venken, K.J.T. et al., 2006. P[acman]: a BAC transgenic platform for targeted insertion of large DNA fragments in D. melanogaster. *Science (New York, N.Y.)*, 314(5806), pp.1747–51.

Venken, K.J.T. & Bellen, H.J., 2007. Transgenesis upgrades for Drosophila melanogaster. *Development (Cambridge, England)*, 134(20), pp.3571–84.

Wang, Y. et al., 2013. The Role of Snail in EMT and Tumorigenesis. *Current cancer drug targets*, 13(9), pp.963–72.

Wang, Y., Liu, F. & Wang, W., 2012. Dynamic mechanism for the transcription

apparatus orchestrating reliable responses to activators. *Scientific reports*, 2, p.422.

Weil, T.T., Parton, R.M. & Davis, I., 2010. Making the message clear: visualizing mRNA localization. *Trends in cell biology*, 20(7), pp.380–90.

Zaret, K.S. & Carroll, J.S., 2011. Pioneer transcription factors: establishing competence for gene expression. *Genes & development*, 25(21), pp.2227–41.

Zeitlinger, J. et al., 2007. Whole-genome ChIP-chip analysis of Dorsal, Twist, and Snail suggests integration of diverse patterning processes in the Drosophila embryo. *Genes & development*, 21(4), pp.385–90.

Zhang, H., Levine, M. & Ashe, H.L., 2001. Brinker is a sequence-specific transcriptional repressor in the Drosophila embryo. *Genes & development*, 15(3), pp.261–6.

Zhao, R. et al., 2011. Gene bookmarking accelerates the kinetics of post-mitotic transcriptional re-activation. *Nature cell biology*, 13(11), pp.1295–304.

Zinzen, R.P. & Papatsenko, D., 2007. Enhancer responses to similarly distributed antagonistic gradients in development. *PLoS computational biology*, 3(5), p.e84.